Crystal mush processes and crustal magmatism

Madeleine C.S. Humphreys[1†], Olivier Namur[2†], Wendy A. Bohrson[3], Pierre Bouilhol[4], George F. Cooper[5], Kari M. Cooper[6], Christian Huber[7], C. Johan Lissenberg[5], Eduardo Morgado[8], Frank J. Spera[9]

[1] Department of Earth Sciences, Durham University, Durham, UK
[2] Department of Earth and Environmental Sciences, KU Leuven, Leuven, Belgium
[3] Department of Geology and Geological Engineering, Colorado School of Mines, Golden, Colorado, USA
[4] Université de Lorraine, CNRS, CRPG, Nancy, France
[5] School of Earth and Environmental Sciences, Cardiff University, Cardiff, UK
[6] Department of Earth and Planetary Sciences, University of California Davis, Davis, CA USA
[7] Department of Earth, Environmental & Planetary Sciences, Brown University, Providence, Rhode Island, USA
[8] Escuela de Geología, Universidad Mayor, Providencia, Santiago, Chile
[9] Dept of Earth Science, University of California Santa Barbara, Santa Barbara, CA USA

[†]**madeleine.humphreys@durham.ac.uk**

[†]**olivier.namur@kuleuven.be**

Much of Earth's magma is stored in the form of extensive crystal mush systems, yet the prevalence of physical processes operating within mushes and their importance in volcanically active regions remain enigmatic. In this Review, we explore the physical properties and key processes of crystal mush systems and highlight how differences in the prevalence of these processes through space and time could be generated through the initiation, evolution and decline of volcanic systems, modulated by heat supply and loss. Disaggregation of mushes results in crystal mush material being mobilised or entrained into lavas and erupted, and presents opportunities to define the timescales and chemistry of some mush processes in volcanically active regions. The diversity of lengthscales on which mush systems can be observed presents difficulties in integrating data and interpretations across different fields. Advances in understanding will require improved integration of thermodynamics, textural analysis, geochemistry, modelling and experiments, as well as inputs from adjacent fields such as porous media dynamics,

engineering and metallurgy. Such advances will ultimately lead towards improved hazard evaluation at active and dormant volcanic systems.

Key points

1. All magmas transition through a mush stage during solidification, when there is an interconnected solid framework that can transmit stress, with an interconnected liquid in the pore spaces.

2. Long-lived crystal mushes are the site for enrichment, segregation and deposition of many mineral deposits, are important for productive geothermal systems. Mush instability is closely linked to volcanic eruption

2. Mush physical behaviour depends primarily on its porosity, melt viscosity, permeability, and crystal shape and size distribution. These properties may be highly heterogeneous across different lengthscales.

3. Cumulates represent the crystalline residue left over after segregation of crystals or extraction or migration of silicate melt during igneous differentiation. They are complementary to erupted magmas

4. Melt migration in crystal mushes can occur by grainscale porous flow or channelisation. Reactive melt migration can affect crystal mush porosity, permeability and composition, and may thus impact chemical evolution.

5. Crystal-melt segregation is enhanced in thermally mature crust. Increased migration, reaction and extraction of melt from the mush is expected in thermally mature volcanic systems, leading to mushy crystal cargo

6. Regional tectonics impact the balance of magma intrusion to buoyant ascent. Mushes in cool and wet settings involve have persistent residual melt and more effective melt segregation

Glossary terms:

Rheology – the study of material deformation and flow; *force chain* – a network of linked particles that carry more than the average load in a mush; *igneous differentiation* – any process by which magmas can change their bulk composition; *diffusion chronometry* – the process of extracting time information about magmatic processes from diffusive changes in chemical gradients; *loosely packed mush* – a loose aggregate of solid particles that can be densified if the particles are rearranged; *maximum packing* - a dense packing of particles that cannot be densified without deformation of the particles; *Rayleigh number* – a dimensionless number that describes the ratio between thermal buoyancy and diffusion, and thus the likelihood of convection; *percolation threshold* – the porosity that marks the end of percolative flow through a porous medium; *primocryst* – a crystal formed in the early stages of fractionation that forms part of the crystal mush framework; *rejuvenation* – the process of mobilising mushy material by adding heat or changing porosity; *entrainment* – the process of incorporating mushy material

as crystal cargo in ascending magmas; *assimilation* – the process of incorporating surrounding crust into magma; *adcumulate rocks* – rocks dominated by unzoned, interstitial overgrowths of the primocryst phases with minimal amounts of trapped pore material.

Introduction

Volcanic systems are the outward expression of plate tectonics and heat loss from the Earth, producing magma storage reservoirs and transport pathways that contain crystal mush: regions of molten rock containing with a crystal framework and varying amounts of melt and fluid[1]. Crystal mush processes (i.e., solidification, remelting or physical separation of crystals and silicate melt in mushes) govern igneous differentiation in all geological scenarios where partial melt is present, from deep mountain building environments, through subduction systems, to mid-ocean ridges and ocean islands. Geophysical information (such as seismic velocity, tomography, gravity or magnetic data) can be used detect the presence of silicate melt, however observations typically identify only relatively small quantities of melt within the crust [e.g. ≤15%[2–4]]. This has driven the paradigm of magma storage as mushes, with stress-bearing crystal frameworks and an interstitial melt network[5–8]; melt-rich bodies are ephemeral[8]. Crystal mush can be defined as a super-solidus rock with a largely interconnected melt phase within a continuous, crystal-rich framework[7,9] and variable fluid content (**Figure 1**). There are extreme changes in chemical and physical properties with crystal fraction[1], such as temperature, melt composition, density, tensile strength, and seismic velocity (**Figure 1**), and the properties of the solid crystal framework control the overall rheology [**G**] of the mush[7–9]. Although part of a continuum from fully liquid to fully solid, magma can be defined as a melt with solid crystals (± fluids) in suspension where the magma rheology is largely controlled by the continuous melt phase[7,9,10]. Partial melting of the crust, through regional or contact metamorphism, also results in the formation of mushy rocks[9], and the definition of crystal mush can be applied equally to crystallisation or partial melting[9,11]. Here, we focus more on crystallisation, but we do not intend to imply a one-directional process. Long-lived mush systems might undergo many iterations of crystallisation, resorption and recrystallisation[12,13], and partial melting of the crust can be a crucial part of magma generation and differentiation[9,11].

Mushes provide a window into multistage crustal magmatic processes that are not decipherable from melts alone. They reflect the heat and mass balance from mantle to crust and are intrinsically linked to geophysical data that can be inverted to image magma storage and transport zones. They give insights into the timescales and mechanisms of system change in the lead up to eruptions, and therefore represent a route towards anticipation of future eruptions.

In this Review, we examine mush processes in crustal magmatic systems across space and time as related to tectonic setting, the evolution of volcanic systems and the precursors to volcanic eruptions. We discuss the different strands of evidence that are used to constrain the occurrence of mush, and summarise the physical and chemical processes that operate during mush formation, rejuvenation and eruption. We evaluate the relative importance of these processes in the context of the evolving thermal maturity of volcanic systems and across different tectonic settings, and discuss how this links to the timescales obtained by radiometric dating or diffusion chronometry of erupted crystals. We conclude that advances in understanding mushes are likely

to arise by improving how we integrate evidence from petrology, geochemistry, geophysics, analogue experiments and dynamical numerical models, across diverse spatial scales.

Evidence and importance of crystal mushes

In order to understand geodynamics, rates of magma transport, the extraction of partial melts from their source, or the timescales of volcanism and crust formation, we must understand how materials are formed and processed through crystal mushes. Because a cooling magma spends most of its lifetime as mush[14], the timescales of magma generation and extraction are intrinsically linked to the physics and flow behaviour (rheology) of multi-phase systems. Igneous differentiation involves changes in melt chemistry as well as physical properties, therefore mush processes are also critical for generating the chemical enrichment required to form many kinds of mineral resources including deposits of chromite[15], rare earth elements[16], platinum group elements[17] and copper[18]. In terms of natural resources, active convection of melt within mushes is important for generating the high heat transport rate required for efficient geothermal systems[19]. Finally, the presence of silicate melt affects the strength, elastic properties and strain partitioning behaviour of the crust, so understanding the formation, behaviour and solidification of mush is key to linking surface geophysical observations to magmatic processes in the crust[20].

The presence of crystal mush in igneous bodies is an inevitable consequence of solidification or thermal equilibration of magma within the crust across all tectonic settings; magma solidifies by progressive crystallisation and must therefore pass through a mushy state. In addition to multi-parametric geophysical evidence[21] and numerical modelling of crustal thermal structure[22], snapshots of crystal mush solidification are represented by melt-bearing nodules[23–25], plutonic enclaves[26–28], and crystal clots and glomerocrysts[29] that are brought to the surface by magma during eruptions from arc volcanoes[30] to mid ocean ridges[31]. In these and plutonic rock samples, grain-scale textures and geochemistry can be used to define crystallisation processes, estimate crystal fractions and infer the occurrence of melt convection, compaction or mush disaggregation within the crystal mush. For example, films of interstitial plagioclase in gabbro indicate the final stages of crystallisation and the formation of grain-boundary symplectites replacing primocrysts reflects localised reaction with migrating late-stage liquids[32]. In arc gabbro xenoliths, hornblende overgrowth on clinopyroxene primocrysts **[G]** is evidence of reactive melt percolation by evolved hydrous melts within the mush[28].

Mushes have also been sampled directly by drilling programmes in lava lakes[33] and during exploration for geothermal resources[19], showing progressive changes in crystal content, melt chemistry, mineralogy and physical properties (**Figure 1**). These changes are reproduced by laboratory experiments seeking to generate mush by holding sampes of basalt at super-solidus temperatures in a thermal gradient[34].

Evidence for larger-scale dynamic mush processes such as differentiation, sedimentation, localised deformation or melt extraction can be found in meso-scale plutonic rock fabrics[9] and bulk and mineral chemistry, including individual intrusions as well as exhumed sections of arc or ocean crust. For example, in the Searchlight Pluton, Nevada, large-scale mapping, geochemistry and high-precision geochronology evidence the extraction of evolved residual liquid from crystal mush to feed overlying leucogranite sills and volcanic eruptions[35]. Syn-

magmatic mush faulting and slumping is exemplified in steep mushy sidewalls in the Skaergaard intrusion[36] and in the Sierra Nevada[37].

Crystal mushes and cumulate formation

Cumulates are the crystalline residue left over after segregation of crystals and extraction or migration of silicate melt during igneous differentiation and their compositions. Cumulates represent a record of geochemical differentiation that is complementary to erupted magmas and is present in exposed plutons, ophiolites, deep crustal transects and as enclaves in volcanic eruptions[27,38,39]. Mineralogically and chemically, cumulates do not represent a bulk melt or magma composition; the solid phase is over-represented relative to the liquid, either as a result of expulsion or (re)moval of interstitial mush liquid, or by differential movement of crystals[40]. We summarise below some of the general mechanisms for forming cumulate mushes and their signatures in natural rocks, before reviewing the geochemical and physical consequences of those processes.

Crystal settling – Crystals can be separated from liquid by settling. For a single crystal, settling depends on size, the density contrast between solid and melt, and on viscous drag between melt and crystal (which depends on melt composition, crystal shape[41] and orientation). However, for abundant crystals, crystal-crystal interactions become important and tend to slow down the migration of crystals[42–44]. Crystal interactions during settling of dense suspensions can generate layers defined by crystal size and density[45–47], can lead to internally differentiating mush packets linked to ore mineralisation[17] and may lead to density instabilities that result in crystal-laden plumes[44,48,49]. These complex interactions affect meso-scale properties of crystal mushes such as size distribution and phase abundance[47], and are implicated in the formation of some metal-rich ore horizons[50].

Consolidation of the crystal mush – A loosely aggregated mush is not at its maximum packing **[G]** density, so melt can be segregated if crystals are consolidated (repacked) into a more efficient spatial arrangement (also termed 'mechanical compaction'[51–53]) by being translated and rotated under gravity or during shear deformation (**Figure 2a, b**). In a loosely packed mush, melt segregation is dominated by frictional interactions between crystals[54]. These interactions can lead to the formation of force chains **[G]** between neighbour crystals that localize stress accumulations and deformation within the mush[55]. High-temperature and analogue experiments[50,56,57] and field and petrological studies on melt loss in shallow to mid-crustal intrusions[58] suggest that porosity **[Box]** can be reduced by up to tens of percent by mechanical consolidation, but this is limited to crystal fractions ≤ 0.7[53]. This process is hard to discern in nature as it leaves little textural signature, except that a foliation should develop[59] (**Figure 2b**) with a strength dependent on crystal shape and the extent of melt loss as estimated by trace element mass balance[38,53,60,61]. Once the maximum packing has been reached, remaining melt can only be expelled by viscous compaction[53] (**Figure 2c**).

Viscous compaction of the crystal mush – In densely packed mushes, further melt extraction occurs by pressure-solution (i.e. dissolution-reprecipitation) processes and by grain boundary diffusion creep[53,62,63]. These cause viscous deformation of the crystal framework, driven by local shear deformation and the density contrast between melt and crystal phases[63–66]. Resistance to

compaction is dominated by viscous drag between the expelled melt and the crystal framework, as well as by the high effective viscosity of the matrix[64,65]. Progressive textural equilibration between crystals and melt (**Box**) leads to an interconnected melt network[67], which is essential for melt extraction[62,63,68].

The thickness of the deforming mush layer can be described using the compaction lengthscale[48,64,65] (**Figure 2d**), which is expected to range from meters to hundreds of meters, depending on melt composition (which affects its physical properties) and the processes controlling mush compaction[48,65,69]. When the mush is highly permeable (and/or the viscosity of the crystal framework is high), the compaction length can be large compared to the thickness of the mush layer, and in that scenario, compaction is limited only by the deformation rate of the crystal framework. This scenario is valid for thin mushes (metres to 10s of metres, depending on melt fraction and melt composition). In contrast, in thick mushes (100s to 1000s metres) the compaction length is significantly smaller than the mush layer thickness and compaction is controlled by both the deformation of the crystal framework and the mush permeability[64,65,69]. In general, compaction should be favoured in long-lived, thick mushes where the density contrast between crystals and melt is high (see **Mush processes and thermal maturity**).

Whether melt can be segregated from a mush by repacking, or involves grain boundary diffusion processes, depends on the competition between compaction rate and cooling (crystallization) rate. Mid- to upper-crustal silicic intrusions show an upper bound for melt loss in their cumulate roots that corresponds roughly to their expected maximum packing, suggesting that consolidation (repacking) controls melt loss in these systems[53,70]. This inference is consistent with an experimentally inferred decrease in compaction rate of 3-5 orders of magnitude between consolidation and viscous deformation[53,57]. These processes merit further study, both because they represent the early stages in the extraction of a potentially eruptible melt that can feed surface volcanic activity, and because they affect the formation of economic resources such as chromitites[50].

Viscous compaction may be identifiable through textural signatures such as undulose extinction, low-angle grain boundaries and mechanical twins[27,71] (**Figure 2e**). These signatures arise from free dislocations that form in response to stress. Pressure-solution can result in truncation of grains, formation of sutured or lobate grain contacts, and compositionally distinct overgrowths on favourably oriented crystal faces[27,71–73]. Deformation textures are relatively common in large plagioclase- or olivine-rich cumulate bodies[74–76] and can be shown to have formed when melt remained present[71,73]. Evidence of melt-present deformation is also present in smaller, lower crustal and oceanic gabbros[75,77]. However, there remains disagreement over whether these features are unambiguously linked to compaction driven by the overlying crystal mush, or to external tectonic drivers[71,75,78].

Melt convective migration within the mush – Crystal settling, mechanical consolidation and viscous compaction are all processes that act on the mush framework, however the chemistry and differentiation of the mush system can also be affected by processes operating on the melt, including convective circulation. In most magmatic systems, melts are less dense than their surrounding crystal framework and evolve towards even lower melt densities. The buoyant interstitial melt can therefore be continuously expelled from the crystal mush through convective separation, and replaced in the pore space by circulating melt from the resident magma body[79,80]. This process, termed compositional convection because the density instability

arises from compositional changes, enables the interstitial melt to maintain a constant composition[79,81] and can lead to formation of crystal overgrowth rims of constant composition[74] (**Figure 2f**). Thermal or compositional convection of interstitial melt within the mush occurs when the Rayleigh number [G] for the mush exceeds a critical value (approx. 25-80[80,82]), depending on factors including the contrast in density between phases within the mush, the permeability and thickness of the mush and the melt viscosity[79]. Compositional convection within a crystal mush requires a mush thickness of 100s meters[80] and relatively high permeability, even for less viscous hydrous melts[83]. The textural signature of compositional convection in cumulates includes mesoscopic pipe structures, which may represent convective return flow[83,84] and adcumulate rocks (i.e., those dominated by unzoned, interstitial overgrowths of the primocryst phases with minimal amounts of trapped pore material[74,85].

Volatile percolation and filter pressing – In addition to convective melt migration, volatiles may also percolate within the mush pore spaces. The behaviour of volatiles in a crystal mush is important because they significantly impact buoyancy and can be significant carriers of metals[86]. As the mush solidifies, volatile exsolution is increasingly favoured because volatiles are typically incompatible and their concentration therefore increases with differentiation. Volatile exsolution is most likely near the top (lower pressure) or in the more evolved parts of mush systems[87]. Bubble nucleation and growth creates a volume change that acts as a pressure source and has been proposed as an efficient means to expel melt: this is termed gas filter pressing[88–90]. The large positive buoyancy of exsolved magmatic volatiles allows them to migrate through crystal mushes[91,92]. The efficiency of volatile transport increases with crystal fraction[91,92] and with the ratio of bubble size to crystal size[89,93], and is expected to be more important in subduction systems with abundant volatiles. However, much volatile transport occurs in the form of viscous fingers[94,95], which significantly limits the amount of melt that can be displaced. Hence, overall, gas filter pressing is not an effective way to facilitate melt loss and the formation of cumulates[52], although it could be an important means of redistributing fluid-mobile elements towards regions of ore deposition[86].

To summarise, cumulates are formed when melt and crystals are segregated from each other or when differentiation occurs through physical processes that act within the mush. Crystal-melt segregation results in igneous differentiation and spatial redistribution of incompatible or fluid-mobile elements, and can yield eruptible melt. This leads to generation of evolved magmas and may give rise to ore mineralisation.

Consequences of melt migration

The convective circulation of interstitial melts relative to their crystal framework (above) has been relatively well studied, particularly for layered cumulates in dry tholeiitic mush systems. However, migration of melt through a mush framework need not be locally convective. Non-convective migration is thought to be a key driver of differentiation and crystal-melt segregation across chemically diverse mush systems[96,97]. In this section, we review the physical nature of

melt migration, explore some of its chemical consequences, and cover feedbacks between melt migration and mush porosity.

Pervasive vs channelised melt migration - The rate of porous melt migration depends on mush permeability, melt density and viscosity, and on the pressure gradient driving flow. Crystal mushes are expected to show variations in porosity and permeability **[Box]** and composition on a range of scales (10^{-3}-10^{3} m), based on the combination of small-scale compositional changes (or 'layering' *sensu lato*) and cm- to km-scale variations seen in many plutonic rocks[74,98,99]. Variations in mineralogy, texture and crystal packing characteristics **[Box]** can create variations in melt fraction on a range of lengthscales, giving rise to variable permeability. The variation of melt fraction with temperature also depends on bulk composition, pressure and volatile (H_2O) contents[100], which leads to further spatial variability. As a result, the style of melt migration is expected to vary.

Many porous systems have two scales (modes) of porous flow, with pervasive, grain-scale porous flow and larger-scale, higher porosity features such as channels. Channelised flow is typical of industrial packed beds as well as natural systems such as the partially molten mantle, where structures such as narrow channels and variable melt compositions can spontaneously develop[9,101] (**Figure 3**). Similar channel features also form in crystal mushes, for example, during melt-solid reaction[102–104], compositional convection[84] or fluid infiltration[91]. Channelisation can also develop dynamically during flow through the porous mush, and this generally requires either reactive flow (see below, i.e, partial dissolution leading to reactive infiltration instabilities[101,105,106] or multiphase (immiscible) flow leading to viscous or capillary fingering[95,107] (**Figure 3**). The scale of channelised features is commonly intermediate between the thin section and the outcrop scale, which may hamper the textural recognition of its effects, and consequently cause difficulties in understanding the extent of channelization and application of modelling interpretations.

Buoyancy-driven melt migration may lead to instabilities in the form of melt-rich lenses[108,109], which can travel through the mush as porosity waves[48,96,108,110]. Such melt-rich lenses could be linked to rapid melt transport through, extraction from, or even creation of, magma reservoirs[48,96,97,111]. Hence, slow (grain-scale) and fast (channelised) transport mechanisms may be physically linked, and together control melt distribution and extraction. This provides a potential mechanism to understand magma formation timescales by drawing together chronological constraints and physics (*see* **Mush Disaggregation and Eruption***)*.

The impact of deformation - In regions of active tectonism, deformation can significantly enhance melt flow and segregation[112]. Key to this is dilation of the mush, which occurs when closely packed mush framework grains are forced apart in order to move past each other, resulting in dilation (volume increase) of the pore spaces[55,111–113]. This locally reduces the pressure in the interstitial melt and can suck in melt from surrounding areas[112,114,115]. This effect can lead to migration of melt away from grain boundaries normal to the maximum compressive stress, and into films or channels parallel to maximum compressive stress[55,114,116]. This migration is consistent with results from modelling, which show that tectonic extension favours vertical melt extraction[22,117]. This is reflected in short timescales for melt transfer in extensional settings[112,118–120] and may also explain the more differentiated chemistry of magmas associated with upper crustal compression than those associated with upper crustal extension[120]. Thus,

shear deformation can lead to local crystal-liquid segregation[114,121] and larger-scale differentiation in both mafic and felsic[9,38] systems.

Regardless of the mechanism for porous melt migration, the degree of textural equilibration between crystals and melt[67] is important, as this affects the solid-melt dihedral angles and therefore controls the connectivity of the melt phase and the melt transfer rate. This is explored later in **Mush processes and crustal thermal maturity.**

Reactive melt percolation - Much recent work has focused on the crystal-melt reactions that can accompany porous flow, because these might have significant implications for melt evolution[96,111,123,124]. These reactions might occur either when a more evolved mush is replenished by more primitive melt[39,125,126] or during the migration of more evolved interstitial melt into a more primitive crystal mush[103,123].

If a replenishing melt is undersaturated in a phase present in the mush, this triggers partial dissolution and results in melting and increased mush porosity[111,127–129] (**Figure 3a**). For example, pyroxene-saturated basaltic melts migrating through olivine-bearing mush[102,130], or amphibole-saturated melts migrating through anhydrous assemblages[28,131] both result in partial dissolution. Even if the migrating melt is saturated in the same phases present in the mush, the incoming melt is unlikely to be in chemical equilibrium with these phases (e.g., anorthite content in plagioclase, Mg# in ferromagnesian phases), resulting in changes in major, trace element and isotopic composition of relict cores and new phases[103,126,129,131–134] through dissolution-reprecipitation.

Diffusive exchange is effective for fast-diffusing elements (e.g. Fe-Mg), and has been called upon to explain compositional trends recorded in plutonic rocks[102]. Given sufficient time, the crystal mush may buffer the composition of the melt for fast-diffusing elements, but not for slower-diffusing elements, leading to compositions trends that are inconsistent with fractional crystallisation[102,125] (**Figure 3b**). Recrystallisation can occur in experiments with run times of 6 hours[135], indicating that these reactions can proceed quickly, at least on the small lengthscales/ grainsizes of experimental charges. If buffering goes to completion for major elements, then this mineral-melt equilibrium may be used for geobarometry and so constrain the depths of mushy reservoirs[136].

Textural evidence for reactive flow typically includes the presence of relict cores and new rim compositions, however, this can be difficult to distinguish from some peritectic reactions, which occur in a closed system[137,138]. For example, amphibole appears during the differentiation of wet arc melts via reaction with clinopyroxene and olivine[103,137,139,140]. More work is needed to define how melt-mush reactions locally alter melt composition, porosity and permeability.

Crystal-melt reactions during porous flow also affect the porosity of crystal mush, and thus have implications for melt transport and accumulation as well as mush stability. Thermodynamically-constrained models for mafic systems show that, generally, recharge with primitive melt leads to net dissolution of mush phases and hence an increase in porosity[125,134]. For many scenarios of reactive flow of already-differentiated, relatively low-temperature interstitial melts in mafic crystal mush, modelling suggests that the ratio of assimilation to crystallisation is close to unity, indicating that porosity is maintained[134]. However, where plagioclase forms a large proportion of the reacted assemblage, porosity might decrease during the migration of evolved melts, depending on temperature[134]. Nonetheless, the rock record preserves evidence of reactive melt

percolation from the micron scale in the Rum Layered Intrusion, Scotland[141] to at least the meter scale in the deep arc and oceanic crust[103,142]. Reactive flow can affect much porosity without significant changes in temperature[96,129], resulting in the formation of melt-rich lenses and potentially leading to mush destabilisation and eruption. Overall, the porosity and permeability evolution of mush systems represents an intersection of numerous complex physical and chemical factors, and an integrated observational, experimental and modelling approach is required to understand it more fully.

Crystal mush disaggregation and eruption

Volcanic eruptions occur when the internal pressure of the magma reservoir exceeds the external lithostatic pressure or the tensile strength of the host rock[143], and when the viscosity of the stored magma is low enough to allow flow, which typically has been assumed to require a melt-dominated magma[14]. Evidence from geochronology and mechanical understanding of mush behaviour suggests that crystal mushes remain in a largely non-eruptible state for most of their lifetime[144–146]. This rheologically locked crystal framework, with interstitial melt, is not eruptible until the mush is rejuvenated or reactivated, which permits the wholesale eruption of crystal-rich mush or extraction of melt-rich magma from mush reservoirs.

Possible mush rejuvenation mechanisms - Mush rejuvenation could occur through mechanisms that are either internal or external to the reservoir [96,97]. In the case of rejuvenation by external recharge, a hotter magma is intruded at the base of (or within) a mush and reactivates and weakens the crystal framework through partial melting[127,147,148]. Rejuvenation is limited by the inefficiency of heat transfer[149,150] and is strongly dependent on mush and magma composition, including volatile content[148]. Nonetheless, there are many examples where mineral chemistry and thermometry indicate that heating has taken place shortly before eruption, which is commonly inferred to have been caused (or immediately preceded) by replenishment and wholesale mush disaggregation[151–153]. Heterogeneous mushes may contain melt-rich layers as a result of intrusion[128] or due to buoyancy-driven porous flow instabilities (see ***Pervasive vs channelised melt migration***). In these cases, mush disaggregation could occur through Rayleigh-Taylor instabilities involving descent of crystal-laden plumes (see ***Crystal Settling***) into the melt[49,154] (**Figure 4a**). Percolation of exsolved hot volatiles through the crystal mush has been suggested to enhance both heat transfer and buoyancy instabilities[91,110,149,155].

Mush rejuvenation through internal mechanisms could include nucleation of bubbles within the crystal framework due to second boiling[87] or destabilisation of a mush with volatile-rich layers[91,150,153,156]. Migration through the mush of melt-rich porosity wave instabilities could result in locally increased melt fraction (i.e. mush disaggregation) without requiring any external forcing[96,97]. In wet felsic systems, reactive melt flow could also increase mush porosity, to the point where the crystal mush might unlock and allow eruption[157,129]. Even in systems where the mush is not significantly disaggregated, melt extraction through dyke generation is efficient in reservoirs within a crystallinity window of ~50–70 vol.%, which could lead to mush derived crystal-poor samples. Any of these events leading to destabilization and disaggregation

of the crystal mush could be a trigger for eruptions, with remnants of parental mushes entrained into erupted magmas (**Figure 4b**).

The crystal cargo - The impact of mush reactivation is to incorporate crystals, potentially from different locations within a mushy reservoir with different origins and histories, into erupted magma as crystal 'cargo'[158]. Whole-rock compositions mask geochemical indicators of mush disaggregation as they represent a mixture of diverse crystal cargoes and melt(s). However, the recognition of the diversity of crystals in erupted magmas has provided petrological evidence for the paradigm shift towards mushy storage systems. Firstly, plutonic or cumulate assemblages either brought to the surface as xenoliths and glomerocrysts or present in exposed crustal sections, show that crystal-rich mush zones are present within magmatic systems[24–27,159–162]. Within many magmas, disequilibrium mineral textures, such as sieve textured cores and strongly reversed zoning in crystal rims[29,31,35,163], and evidence for peritectic reactions or metastable phases[164,165], have been used to infer that the crystals originated in a mush that was subject to thermo-chemical rejuvenation and incorporation into an eruptible magma (**Figure 4b**). These crystals are termed 'antecrysts' as they spent most of their life within the mush system and did not originate from the final erupted magma. Elemental and isotopic variations within crystals also demonstrate influx of new melt or transfer of solids into new environments. Evidence for such processes in the crystal cargo includes reverse zoning, trace element zoning that is inconsistent with major-element partitioning, and crystal-scale isotopic disequilibrium between crystals and host melt (e.g. Pb isotopic compositions of sanidine[166]; in situ Sr isotopes in interstitial plagioclase[141]; and Hf and O isotopic and trace elemental compositions of zircon[35,167] also demonstrate influx of new melt or transfer of solids into new environments, during crystallisation).

The crystal cargo represents a toolbox to calculate the timescales of storage, rejuvenation, or disruption of the mush and release of free crystals into an eruptible magma. Radiometric ages of minerals date crystallization times, and typical pre-eruptive residence of crystals in volcanic rocks are thousands of years (major phases) to tens of thousands of years (zircon)[168]. In contrast, methods to quantify rejuvenation times include Ar/Ar dating of feldspar[169], computational modelling[148] and diffusion chronometry. The latter provides a means to investigate a range of timescales: from years to hundreds of thousands of years (using quartz[170] or plagioclase[171]); hundreds to thousands of years using sanidine[172]; years to thousands of years using clinopyroxene[173] or orthopyroxene[119,169]; minutes to months using Fe-Ti oxides[174], although the application of diffusion chronometry typically relies on there having been enough sufficient time between rejuvenation and eruption to permit mineral rim growth. What is apparent using these techniques is that the estimated timescales of rejuvenation can be rapid (order of days in many mafic systems or tens of years to thousands of years in more silicic systems). The rapid timescales deduced from diffusion chronometry are commonly at odds to the protracted timescales estimated for the establishment of the whole magmatic system[144–146]. This contrast between long storage timescales and short rejuvenation timescales recorded in the crystal record has been ascribed to cold mush storage[144,145] with little interstitial melt. However, some systems may be characterised by larger melt fractions, as has been argued on the basis of combined zircon thermometry and geochronology[175]. Alternatively, the application of diffusion chronometry relies on experimentally constrained diffusion coefficients; current lack of agreement between experimental studies means that diffusion timescales could reflect magma reservoir build up rather than eruption-related processes[176,177]. Otherwise, the apparent disparity in timescales may point towards an additional external mechanism for melt extraction, such as

473 the regional stress field and/or pre-existing tectonic structures in active regions such as New
474 Zealand[119,170,178] and the Southern Volcanic Zone of the Andes[120,179]. Improving quantitative
475 constraints on both temperature and timescales, for example through modelling approaches, will
476 help to define the storage conditions of the crust and magmatic reservoirs throughout their
477 lifetimes, and can help provide an integrated perspective on all steps involved in mush
478 rejuvenation[148].

479

480 **Crystal mush processes and crustal thermal maturity**

481 Motivated by the need to understand the future eruptive behaviour of volcanoes, we need to
482 understand more about volcanic system lifetimes, patterns of intrusion and eruption, and the
483 timescales and lengthscales of melt and crystal residence in the crust. The rejuvenation
484 processes outlined above are crucial for allowing the mush system to evolve chemically. Key
485 factors affecting the prevalence and effectiveness of mush processes include the thermal state
486 of the crust, tectonic setting, and the mass and thermal balance of magma addition through
487 intrusion into the crust. Both the textural character of the mush framework (**Box**) and the
488 composition of the mush melt(s) respond to crustal thermal state and can also themselves limit
489 mush processes. Below we review how these controls affect mushes across the lifetime of a
490 crustal volcanic system, before considering the impact of regional tectonic environment.

491 ***The thermal state of the crust -*** The thermal state of the crust, and thus the cooling rate and
492 crystal content of igneous intrusions, is controlled by the balance of heat inputs (from intrusion
493 of mantle-derived melts, release of latent heat[125,129,180] or redistribution of partial melt
494 throughout the upper and lower crust[22,181]) and outputs (including conductive cooling away from
495 the magma and hydrothermal circulation[180,182]. The thermal state of the crust therefore primarily
496 depends on crustal thickness[183], mantle-derived melt fluxes and regional tectonics[22], and the
497 distribution of radiogenic heat-producing species throughout the crust[184]. The thermal
498 environment controls the cooling rate of intrusions and therefore the amount of time available
499 for mush processes, such as viscous compaction, melt extraction or porous melt migration, to
500 take place. For example, early mafic to intermediate magmatism can thermally prime the crust,
501 extending thermal equilibration times enough to allow segregation of evolved melt that
502 generates silicic plutons[185]. The thermal environment also affects the amount of energy available
503 for assimilation of surrounding crust or remobilisation of older, colder mushes. The crust in
504 volcanically active areas will change in thermal maturity over the lifetime of the whole volcanic
505 system[22,96,97,186,187] (**Figure 5**), so we should expect to see differences in the efficiency of mush
506 processes over those lifetimes, dependent on the thermal state of the crustal reservoir.

507 The textural maturity of the mush is also affected by its thermal state and will progress
508 diffusively towards increasing connectivity of the melt phase[27] (**Box**). Long-lived (mature)
509 mush systems (from 100 kyr to 1-10 Ma[145,146,188]) are expected to tend towards more mature
510 crystal textures and melt geometries (lower dihedral angles[67]). Repeated episodes of heating,
511 resorption and recrystallisation that occur in long-lived mush systems [91,145,146,186] also impact the
512 shapes of crystals in mushes, which evolve towards more equant character, closer to equilibrium
513 (Wulff) crystal shapes[13].

514 ***Thermally immature systems -*** In thermally immature (maturing) systems (**Figure 5a**), each
515 intrusion cools quickly[96,97,186]. Individual events generate packets of crystal mush that are short-

lived, and produce only limited amounts of extracted evolved melt[111], together with only limited local melting and assimilation of the crust[96,187]. The short lifetime of these mushes, less equilibrated textures, and lower overall ambient temperatures in thermally immature crust, together lead to limited opportunity for viscous compaction, mechanical arrangement or porous melt migration in the early stages of a volcanic system (the 'incubation stage' of ref [[96]]). Immature or young systems are unlikely to sustain large upper crustal magma chambers[22,181].

Thermally mature systems - Thermal maturity (**Figure 5b**) is attained for geologically reasonable melt fluxes within ~ 1 Ma[96,111,117,189]. High ambient temperature and high melt flux means that magmatic systems can easily be maintained above the solidus for extended periods of times, perhaps exceeding 10^5 yr[182,190,191]. The smoothly curving grain boundaries and continuous grain boundary melt films of texturally mature mush [**Box**] facilitate effective porous melt migration even at low melt fractions[68,192] and lead to mass transfer and melt differentiation and reactive flow[96,129,174], as recognised in the geological record in deep seated crustal systems[102,103,125]. Thermal maturation leads to increasing extents of crustal assimilation, as seen through modelling[96,111,117] and through isotopic analysis combined with geochronology of mid-upper crustal plutons[193,194].

Many middle to upper crustal reservoirs receive magmatic inputs directly from lower crustal mushes[181,195,196] (**Figure 5b**), and themselves represent long-lived silicic mush systems (e.g. the Altiplano Puna Magma Body[4]). Some upper crustal reservoirs beneath composite volcanoes generate evolved products directly from primitive melt through a long-lived crystal mush[195,197].

Thermally waning systems - The waning stages of magmatic systems (**Figure 5c**) are under-represented in the literature; existing studies suggest these systems experience an overall decrease in heat input, lower mass eruption rates and decreasing magmatic temperatures[188,193,197] and might be associated with a return to more mafic volcanism[111,193,198]. Waning systems may also see relatively more recycling (assimilation) of lower crustal cumulates and residual mushes compared with recharge[199,200]. The temporal progression of magmatic systems is challenging to investigate because in plutonic rocks, preserved magmatic structures could be dominated by the most voluminous or later stages of magmatism; the magmatic record of melt chemistry may also be progressively overprinted and masked by later activity[187].

Extensional vs compressional environments – Coupled with the thermal structure of the crust, regional tectonics play an important role in controlling crystal mush development. For example, extensional tectonics imparts a shear stress on the crust which has been inferred as the driver for rapid vertical melt extraction in extensional settings[112,114,118–120] (see ***The impact of deformation***). Extension also perturbs the geotherm, which increases the extent of melting and allows magma to be advected into the upper crust[22]. Conversely, compressional tectonics inhibit buoyant magma ascent through dyking and therefore enhance magma intrusion[201]. Crustal thickness is closely linked to thermal maturity because ambient temperatures are higher in thick crust[97] and this will lead to enhanced melt-solid differentiation in both deeply stored crystal mushes and in thick crust[183].

Tectonic setting – There are some key differences expected in cool and wet (arc) settings compared with hot and dry (extensional or hotspot) settings. In particular, the relationship between temperature and crystallinity changes strongly for different melt compositions and water contents, and this determines how long residual melt can persist in the system[22] (**Figure 6**). For example, a dry tholeiitic melt could crystallise fully over a temperature interval of <100 °C, whereas a wet andesitic melt could still contain melt after 450 °C of cooling (**Figure 6**).

This means that crystal mush in deep arc crust may persist for longer than crystal mush in a shallow oceanic crust, allowing crystal-melt segregation and viscous compaction and extensive entrainment of older mush material. A water-rich melt is also more easily segregated at a given mush crystal fraction due to its lower viscosity and is more likely to form isolated melt-rich lenses[202]. Finally, the relationship between volatile content and crystal content in a crystal mush impacts whether volatile transport involves isolated inter-crystalline pathways or affects the buoyancy of the bulk mush[91]. This impacts the efficiency of outgassing and therefore potential explosivity of resulting volcanic activity.

Summary and future directions

Crystal mushes are a ubiquitous feature of all crystallising magma bodies, which makes understanding their properties and behaviour an important focus for research into volcanic and magmatic systems. The physical properties of crystal mushes are defined by their pore-scale to metre-scale characteristics, including crystal fraction, size and shape distribution, permeability, and the degree of textural equilibration between crystals and melt (which is intrinsically linked to permeability). Their behaviour is highly complex and involves non-linear feedbacks: mushes are characterised by the flow of heat, momentum and chemical species on a number of simultaneous spatial and temporal scales. To date, theoretical work has typically focused on simple, monodisperse grain shapes, maximally dense grain packings, and frictionless systems. In order to understand the timescales and lengthscales of melt extraction and infiltration processes, and to robustly link field and textural evidence with physics and chemical reactivity, the rheology of natural crystal packings needs to be more completely characterised. Further research focusing on more realistic grain shapes and size dispersions would enable more direct comparisons to natural mush textures, using X-ray tomography or 2D trace elemental geochemical mapping to characterise directly how porosity and permeability evolve as natural mushes crystallise. Improvements to understanding of crystal mush behaviour may also come from engaging with researchers in associated fields such as engineering and metallurgy, where processes such as slurry flow and hot tearing in crystallising alloys are applicable to natural silicate mushes.

Cumulates form where physical processes, such as hindered settling, mechanical consolidation, viscous compaction, compositional convection or gas flow (as opposed to simple *in situ* crystallisation) have caused melt and crystals to segregate. Geochemically, cumulate mushes cannot represent a magma composition. The nature of mush compaction is an area that remains poorly understood but is highly relevant to cumulate formation, mush evolution and melt extraction to form upper crustal volcanic systems. Improving understanding of mush compaction needs a wide-ranging investigation of varied natural plutonic settings. An important goal would be to link chemistry and deformation on length scales from grain-scale to intrusion-scale, with 3D orientation of any zoning or dislocation creep. The onset, spatial extent, and orientation of the compaction likely depends on size, shape and orientations of the crystals in the mush, as well as the temperature and longevity of each system. The relative importance and timescales of compaction, consolidation and melt extraction could be investigated using

numerical modelling combined with novel petrographic and textural analyses of mush structure and crystal defects, for example using Electron Backscatter Diffraction.

An emerging research focus is on the impacts of melt migration through crystal mushes. Here, petrological work demonstrates the incidence of *in situ* reactions involving dissolution and reprecipitation, which is most convincingly demonstrated using changes to the textures and trace element geochemistry of the minerals involved in the reactions. In contrast, modelling studies and rheology work emphasise the importance of larger-scale features such as porosity waves and channelisation that are challenging to capture through petrological analysis. Understanding of reactive melt migration is in its infancy, and many open questions remain. Arguably, the most important question pertains to the timing of reactive flow relative to melt extraction: is reactive flow a fundamental component of melt transport and accumulation, or does it occur predominantly in mush reservoirs as porosity is decreasing and the system is freezing? Similarly, the mechanisms, time scales and chemical effects of reactive flow need to be better constrained. Both aspects are fundamentally important to understanding of the compositional evolution of melts. In order to make progress on these issues, an integrated experimental and theoretical (modelling) framework is required for reactive flow, which can then be benchmarked against natural observations. From a modelling perspective, this requires advances in numerical methods for coupling reaction and transport, and for methods that capture full phase equilibria of natural systems.

The scale of the models is also important: reservoir-scale models should be complemented by grain-scale to meso-scale modelling to capture the full range of complexity in governing processes. Numerical schemes that can incorporate the macro and microphysics will be required, and the outputs need to be integrated with field based observations and petrology. Experimental studies will constrain mechanisms and rates of crystal-melt reactions, providing critical input to models, but advances in thermodynamic treatment will be required to match models and in situ geochemistry. Case studies of plutonic and volcanic systems, combining spatially constrained elemental and isotopic data, can help reconstruct the evolution of porosity and permeability as a function of composition and temperature, and constrain the length scale and time scale of porous flow. Similar advances in adjacent fields, such as aqueous reactive flow in hydrothermal systems, may be adaptable to high-temperature magmatic systems.

Crystal mushes are sampled partly through being disaggregated during later intrusive (i.e., magmatic recharge) events and incorporated into volcanic products. The mechanisms of disaggregation have not been extensively studied but could include a combination of larger-scale fluid dynamical instabilities and local grain-scale remelting/ reaction and infiltration by new melts. Many grain-scale processes will be enhanced by relatively mature, equilibrated textures. The mush-derived crystal cargo can be used to explore the timescales of mush storage, rejuvenation and disruption.

Crystal mushes, mush processes and cumulates can occur, and can be sampled, at a range of lengthscales from tens km (through continuum scale numerical modelling, geophysical observations, geological mapping and bulk rock geochemistry), to um (using crystal-scale textures, geochemistry and pore-scale numerical modelling). However, the diversity in the scale and nature of the observations also poses fundamental difficulties in trying to integrate information from different techniques, because different kinds of information are derived from different scales and at different stages of development of crystal mush systems. Volcanic

systems involve multiple interacting timescales reflecting competing processes across different spatial scales. The effect of varying the thermal maturity of the crust, over long timescales representative of whole volcanic systems, is not well explored, and could help to understand the prevalence of particular mush processes as a function of system life cycle, as well as improve the linkages among petrology, geochemistry, advanced geophysics techniques such as full waveform inversion, dynamics of multi-phase flow, and numerical modelling.

Acknowledgements

MCSH has received funding from the European Research Council (ERC) under the European Union's Horizon 2020 research and innovation programme (grant agreement no. 864923), and also acknowledges support from the UK Natural Environment Research Council (grant NE/T000430/1). MCSH thanks Fabian Wadsworth, Ed Llewellin and members of the mush group at Durham for helpful comments on the manuscript, and Catherine Annen for useful discussions. ON acknowledges support from FWO for multiple projects. ON thanks Marian Holness for very useful suggestions. C.H. acknowledges support from NSF EAR-2021328. WAB acknowledges support from the US National Science Foundation. PB acknowledges funding from INSU and OTElo and fruitful discussions with L. France. GFC is funded by a Royal Society University Research Fellowship 2022. KMC acknowledges support from the US National Science Foundation for multiple projects that contributed to the development of these ideas. CJL was supported by the Natural Environment Research Council. FJS gratefully acknowledges funding by the US National Science Foundation and the US Department of Energy over many years for studies of magmatic systems.

Competing interests

The authors declare no competing interests

Author contributions

All authors contributed to discussion of the content; and to writing, review and editing of the manuscript prior to submission.

References

1. Marsh, B. D. Solidification fronts and magmatic evolution. *Mineralogical Magazine* **60**, 5–40 (1996).
2. Paulatto, M. *et al.* Advances in seismic imaging of magma and crystal mush. *Frontiers in Earth Science* **10**, (2022).
3. Magee, C. *et al.* Magma plumbing systems: a geophysical perspective. *Journal of Petrology* **59**, 1217–1251 (2018).

4. Ward, K. M., Zandt, G., Beck, S. L., Christensen, D. H. & McFarlin, H. Seismic imaging of the magmatic underpinnings beneath the Altiplano-Puna volcanic complex from the joint inversion of surface wave dispersion and receiver functions. *Earth and Planetary Science Letters* **404**, 43–53 (2014).
5. Bachmann, O. & Bergantz, G. W. On the origin of crystal-poor rhyolites: extracted from batholithic crystal mushes. *Journal of Petrology* **45**, 1565–1582 (2004).
6. Annen, C., Blundy, J. & Sparks, R. The genesis of intermediate and silicic magmas in deep crustal hot zones. *Journal of Petrology* **47**, 505–539 (2006).
7. Sparks, R. *et al.* Formation and dynamics of magma reservoirs. *Philosophical Transactions of the Royal society A* **377**, 20180019 (2019).
8. Cashman, K. V., Sparks, R. S. J. & Blundy, J. D. Vertically extensive and unstable magmatic systems: a unified view of igneous processes. *Science* **355**, eaag3055 (2017).
9. Weinberg, R. F., Vernon, R. H. & Schmeling, H. Processes in mushes and their role in the differentiation of granitic rocks. *Earth-Science Reviews* **220**, 103665 (2021).
10. Mueller, S., Llewellin, E. & Mader, H. The rheology of suspensions of solid particles. *Proceedings of the Royal Society A: Mathematical, Physical and Engineering Sciences* **466**, 1201–1228 (2010).
11. Vigneresse, J. L., Barbey, P. & Cuney, M. Rheological transitions during partial melting and crystallization with application to felsic magma segregation and transfer. *Journal of Petrology* **37**, 1579–1600 (1996).
12. Bohrson, W. A. *et al.* Thermodynamic model for energy-constrained open-system evolution of crustal magma bodies undergoing simultaneous recharge, assimilation and crystallization: the magma chamber simulator. *Journal of Petrology* **55**, 1685–1717 (2014).
13. Mangler, M. F. *et al.* Crystal Resorption as a Driver for Mush Maturation: an Experimental Investigation. *Journal of Petrology* **65**, egae088 (2024).

14. Marsh, B. D. On the crystallinity, probability of occurrence, and rheology of lava and magma. *Contributions to Mineralogy and Petrology* **78**, 85–98 (1981).
15. O'Driscoll, B., Emeleus, C. H., Donaldson, C. H. & Daly, J. S. Cr-spinel seam petrogenesis in the Rum Layered Suite, NW Scotland: cumulate assimilation and in situ crystallization in a deforming crystal mush. *Journal of Petrology* **51**, 1171–1201 (2010).
16. Larsen, L. M. & Sørensen, H. The Ilímaussaq intrusion—progressive crystallization and formation of layering in an agpaitic magma. *SP* **30**, 473–488 (1987).
17. Nielsen, T. F. *et al.* The Skaergaard PGE and gold deposit: the result of in situ fractionation, sulphide saturation, and magma chamber-scale precious metal redistribution by immiscible Fe-rich melt. *Journal of Petrology* **56**, 1643–1676 (2015).
18. Buret, Y. *et al.* From a long-lived upper-crustal magma chamber to rapid porphyry copper emplacement: Reading the geochemistry of zircon crystals at Bajo de la Alumbrera (NW Argentina). *Earth and Planetary Science Letters* **450**, 120–131 (2016).
19. Eichelberger, J. Distribution and Transport of Thermal Energy within Magma–Hydrothermal Systems. *Geosciences* **10**, 212 (2020).
20. Mullet, B. & Segall, P. The Surface Deformation Signature of a Transcrustal, Crystal Mush-Dominant Magma System. *JGR Solid Earth* **127**, e2022JB024178 (2022).
21. Iyer, H. M. Geophysical evidence for the locations, shapes and sizes, and internal structures of magma chambers beneath regions of Quaternary volcanism. *Phil. Trans. R. Soc. Lond. A* **310**, 473–510 (1984).
22. Karakas, O. & Dufek, J. Melt evolution and residence in extending crust: Thermal modeling of the crust and crustal magmas. *Earth and Planetary Science Letters* **425**, 131–144 (2015).

738 23. Tait, S. R., Wörner, G., Van Den Bogaard, P. & Schmincke, H.-U. Cumulate
739 nodules as evidence for convective fractionation in a phonolite magma chamber.
740 *Journal of Volcanology and Geothermal Research* **37**, 21–37 (1989).
741 24. Holness, M. B. *et al.* Textures in partially solidified crystalline nodules: a window
742 into the pore structure of slowly cooled mafic intrusions. *Journal of Petrology* **48**,
743 1243–1264 (2007).
744 25. Horn, E. L., Taylor, R. N., Gernon, T. M., Stock, M. J. & Farley, E. R. Composition
745 and petrology of a mush-bearing magma reservoir beneath Tenerife. *Journal of*
746 *Petrology* **63**, egac095 (2022).
747 26. Kiddle, E. *et al.* Crustal structure beneath Montserrat, Lesser Antilles, constrained
748 by xenoliths, seismic velocity structure and petrology. *Geophysical Research*
749 *Letters* **37**, (2010).
750 27. Holness, M. B., Stock, M. J. & Geist, D. Magma chambers versus mush zones:
751 constraining the architecture of sub-volcanic plumbing systems from
752 microstructural analysis of crystalline enclaves. *Philosophical Transactions of the*
753 *Royal Society A* **377**, 20180006 (2019).
754 28. Cooper, G. F., Davidson, J. P. & Blundy, J. D. Plutonic xenoliths from Martinique,
755 Lesser Antilles: evidence for open system processes and reactive melt flow in
756 island arc crust. *Contributions to Mineralogy and Petrology* **171**, 87 (2016).
757 29. Neave, D. A., Buisman, I. & Maclennan, J. Continuous mush disaggregation
758 during the long-lasting Laki fissure eruption, Iceland. *American Mineralogist:*
759 *Journal of Earth and Planetary Materials* **102**, 2007–2021 (2017).
760 30. Arculus, R. J. & Wills, K. J. A. The Petrology of Plutonic Blocks and Inclusions
761 from the Lesser Antilles Island Arc. *Journal of Petrology* **21**, 743–799 (1980).
762 31. Bennett, E. N., Lissenberg, C. J. & Cashman, K. V. The significance of
763 plagioclase textures in mid-ocean ridge basalt (Gakkel Ridge, Arctic Ocean).
764 *Contributions to Mineralogy and Petrology* **174**, 1–22 (2019).

765 32. Holness, M. B., Humphreys, M. C., Sides, R., Helz, R. T. & Tegner, C. Toward an
766 understanding of disequilibrium dihedral angles in mafic rocks. *Journal of*
767 *Geophysical Research: Solid Earth* **117**, B06207 (2012).
768 33. Helz, R. T. Crystallization history of Kilauea Iki lava lake as seen in drill core
769 recovered in 1967–1979. *Bulletin Volcanologique* **43**, 675–701 (1980).
770 34. Lesher, C. E. & Walker, D. Cumulate maturation and melt migration in a
771 temperature gradient. *J. Geophys. Res.* **93**, 10295–10311 (1988).
772 35. Wallrich, B. *et al.* Volcano-pluton connection: Perspectives on material and
773 process linkages, Searchlight pluton and Highland Range volcanic sequence,
774 Nevada, USA. *Earth-Science Reviews* **238**, 104361 (2023).
775 36. Holness, M. B. *et al.* Crystal mush growth and collapse on a steep wall: the
776 marginal border series of the Skaergaard Intrusion, East Greenland. *Journal of*
777 *Petrology* **63**, egab100 (2022).
778 37. Alasino, P. H., Ardill, K. E. & Paterson, S. R. Magmatic faults: Challenges,
779 progress, and possibilities. *Earth-Science Reviews* **260**, 104992 (2025).
780 38. Garibaldi, N., Tikoff, B., Schaen, A. J. & Singer, B. S. Interpreting granitic fabrics
781 in terms of rhyolitic melt segregation, accumulation, and escape via tectonic filter
782 pressing in the Huemul Pluton, Chile. *Journal of Geophysical Research: Solid*
783 *Earth* **123**, 8548–8567 (2018).
784 39. Bédard, J. H. Cumulate recycling and crustal evolution in the Bay of Islands
785 ophiolite. *The Journal of Geology* **99**, 225–249 (1991).
786 40. Vernon, R. & Collins, W. Structural criteria for identifying granitic cumulates. *The*
787 *Journal of Geology* **119**, 127–142 (2011).
788 41. Kerr, R. C. & Lister, J. R. The effects of shape on crystal settling and on the
789 rheology of magmas. *The Journal of Geology* **99**, 457–467 (1991).
790 42. Druitt, T. Settling behaviour of concentrated dispersions and some volcanological
791 applications. *Journal of volcanology and geothermal research* **65**, 27–39 (1995).

43. Schwindinger, K. R. Particle dynamics and aggregation of crystals in a magma chamber with application to Kilauea Iki olivines. *Journal of Volcanology and Geothermal Research* **88**, 209–238 (1999).
44. Suckale, J., Sethian, J. A., Yu, J. & Elkins-Tanton, L. T. Crystals stirred up: 1. Direct numerical simulations of crystal settling in nondilute magmatic suspensions. *Journal of Geophysical Research* **117**, (2012).
45. Namur, O. *et al.* Igneous layering in basaltic magma chambers. *Layered intrusions* 75–152 (2015).
46. Snabre, P., Pouligny, B., Metayer, C. & Nadal, F. Size segregation and particle velocity fluctuations in settling concentrated suspensions. *Rheologica acta* **48**, 855–870 (2009).
47. Bons, P. D. *et al.* Layered intrusions and traffic jams. *Geology* **43**, 71–74 (2015).
48. Wong, Y.-Q. & Keller, T. A unified numerical model for two-phase porous, mush and suspension flow dynamics in magmatic systems. *Geophysical Journal International* **233**, 769–795 (2023).
49. Michioka, H. & Sumita, I. Rayleigh-Taylor instability of a particle packed viscous fluid: Implications for a solidifying magma. *Geophysical Research Letters* **32**, L03309 (2005).
50. Manoochehri, S. & Schmidt, M. W. Settling and compaction of chromite cumulates employing a centrifuging piston cylinder and application to layered mafic intrusions. *Contributions to Mineralogy and Petrology* **168**, 1–20 (2014).
51. Holness, M. B. Melt segregation from silicic crystal mushes: a critical appraisal of possible mechanisms and their microstructural record. *Contributions to Mineralogy and Petrology* **173**, 48 (2018).
52. Bachmann, O. & Huber, C. The inner workings of crustal distillation columns; the physical mechanisms and rates controlling phase separation in silicic magma reservoirs. *Journal of Petrology* **60**, 3–18 (2019).

53. Florez, D. *et al.* Repacking in Compacting Mushes at Intermediate Melt Fractions: Constraints from Numerical Modeling and Phase Separation Experiments on Granular Media. *JGR Solid Earth* **129**, e2024JB029077 (2024).
54. Couturier, É., Boyer, F., Pouliquen, O. & Guazzelli, É. Suspensions in a tilted trough: second normal stress difference. *Journal of Fluid Mechanics* **686**, 26–39 (2011).
55. Bergantz, G. W., Schleicher, J. M. & Burgisser, A. On the kinematics and dynamics of crystal-rich systems. *Journal of Geophysical Research: Solid Earth* **122**, 6131–6159 (2017).
56. Hoyos, S., Florez, D., Pec, M. & Huber, C. Crystal Shape Control on the Repacking and Jamming of Crystal-Rich Mushes. *Geophysical Research Letters* **49**, e2022GL100040 (2022).
57. Renner, J., Viskupic, K., Hirth, G. & Evans, B. Melt extraction from partially molten peridotites. *Geochemistry, Geophysics, Geosystems* **4**, (2003).
58. Hartung, E. *et al.* Evidence for Residual Melt Extraction in the Takidani Pluton, Central Japan. *Journal of Petrology* **58**, 763–788 (2017).
59. Cuetos, A., Dennison, M., Masters, A. & Patti, A. Phase behaviour of hard board-like particles. *Soft Matter* **13**, 4720–4732 (2017).
60. Meurer, W. & Boudreau, A. Compaction of igneous cumulates part I: geochemical consequences for cumulates and liquid fractionation trends. *The Journal of Geology* **106**, 281–292 (1998).
61. Meurer, W. & Boudreau, A. Compaction of igneous cumulates part II: compaction and the development of igneous foliations. *The Journal of Geology* **106**, 293–304 (1998).
62. Cooper, R. & Kohlstedt, D. Solution-precipitation enhanced diffusional creep of partially molten olivine-basalt aggregates during hot-pressing. *Tectonophysics* **107**, 207–233 (1984).

63. Tharp, T. M., Loucks, R. R. & Sack, R. O. Modeling compaction of olivine cumulates in the Muskox intrusion. *American Journal of Science* **298**, 758–790 (1998).
64. Ribe, N. M. Theory of melt segregation—a review. *Journal of volcanology and geothermal research* **33**, 241–253 (1987).
65. McKenzie, D. The generation and compaction of partially molten rock. *Journal of petrology* **25**, 713–765 (1984).
66. McKenzie, D. Compaction and Crystallization in Magma Chambers: Towards a Model of the Skaergaard Intrusion. *Journal of Petrology* **52**, 905–930 (2011).
67. Holness, M. B., Cheadle, M. J. & McKenzie, D. On the use of changes in dihedral angle to decode late-stage textural evolution in cumulates. *Journal of Petrology* **46**, 1565–1583 (2005).
68. Cheadle, M., Elliott, M. & McKenzie, D. Percolation threshold and permeability of crystallizing igneous rocks: The importance of textural equilibrium. *Geology* **32**, 757–760 (2004).
69. Keller, T. & Suckale, J. A continuum model of multi-phase reactive transport in igneous systems. *Geophysical Journal International* **219**, 185–222 (2019).
70. Lee, C.-T. A. & Morton, D. M. High silica granites: Terminal porosity and crystal settling in shallow magma chambers. *Earth and Planetary Science Letters* **409**, 23–31 (2015).
71. Holness, M. B., Vukmanovic, Z. & Mariani, E. Assessing the role of compaction in the formation of adcumulates: a microstructural perspective. *Journal of Petrology* **58**, 643–673 (2017).
72. Boudreau, A. E. & McBirney, A. R. The Skaergaard layered series. Part III. Non-dynamic layering. *Journal of Petrology* **38**, 1003–1020 (1997).
73. Bertolett, E., Prior, D., Gravley, D., Hampton, S. & Kennedy, B. Compacted cumulates revealed by electron backscatter diffraction analysis of plutonic lithics. *Geology* **47**, 445–448 (2019).

874 74. Namur, O. & Charlier, B. Efficiency of compaction and compositional convection
875 during mafic crystal mush solidification: the Sept Iles layered intrusion, Canada.
876 *Contributions to Mineralogy and Petrology* **163**, 1049–1068 (2012).
877 75. Lissenberg, C. J., MacLeod, C. J. & Bennett, E. N. Consequences of a crystal
878 mush-dominated magma plumbing system: a mid-ocean ridge perspective.
879 *Philosophical Transactions of the Royal Society A* **377**, 20180014 (2019).
880 76. Yao, Z., Qin, K. & Xue, S. Kinetic processes for plastic deformation of olivine in
881 the Poyi ultramafic intrusion, NW China: Insights from the textural analysis of a~
882 1700 m fully cored succession. *Lithos* **284**, 462–476 (2017).
883 77. Ferrando, C. *et al.* Role of compaction in melt extraction and accumulation at a
884 slow spreading center: Microstructures of olivine gabbros from the Atlantis Bank
885 (IODP Hole U1473A, SWIR). *Tectonophysics* **815**, 229001 (2021).
886 78. Vukmanovic, Z., Holness, M. B., Stock, M. J. & Roberts, R. J. The Creation and
887 Evolution of Crystal Mush in the Upper Zone of the Rustenburg Layered Suite,
888 Bushveld Complex, South Africa. *Journal of Petrology* **60**, 1523–1542 (2019).
889 79. Tait, S. R., Huppert, H. E. & Sparks, R. S. J. The role of compositional convection
890 in the formation of adcumulate rocks. *Lithos* **17**, 139–146 (1984).
891 80. Tait, S. & Jaupart, C. Compositional convection in a reactive crystalline mush and
892 melt differentiation. *Journal of Geophysical Research* **97**, 6735–6756 (1992).
893 81. Kerr, R. C. & Tait, S. R. Crystallization and compositional convection in a porous
894 medium with application to layered igneous intrusions. *Journal of Geophysical*
895 *Research* **91**, 3591–3608 (1986).
896 82. Sparks, R. S. J., Huppert, H. E., Kerr, R., McKenzie, D. & Tait, S. R. Postcumulus
897 processes in layered intrusions. *Geological Magazine* **122**, 555–568 (1985).
898 83. Petford, N. Porous media flow in granitoid magmas: an assessment. in *Flow and*
899 *Creep in the Solar System: Observations, Modeling and Theory* 261–286
900 (Springer, 1993).

84. Tait, S. & Jaupart, C. Compositional convection in a reactive crystalline mush and melt differentiation. *Journal of Geophysical Research: Solid Earth* **97**, 6735–6756 (1992).
85. Wager, L. R., Brown, G. M. & Wadsworth, W. J. Types of igneous cumulates. *Journal of Petrology* **1**, 73–85 (1960).
86. Vigneresse, J.-L., Truche, L. & Richard, A. How do metals escape from magmas to form porphyry-type ore deposits? *Ore Geology Reviews* **105**, 310–336 (2019).
87. Humphreys, M. C. *et al.* Rapid pre-eruptive mush reorganisation and atmospheric volatile emissions from the 12.9 ka Laacher See eruption, determined using apatite. *Earth and Planetary Science Letters* **576**, 117198 (2021).
88. Pistone, M. *et al.* Gas-driven filter pressing in magmas: Insights into in-situ melt segregation from crystal mushes. *Geology* **43**, 699–702 (2015).
89. Boudreau, A. Bubble migration in a compacting crystal-liquid mush. *Contributions to Mineralogy and Petrology* **171**, 1–17 (2016).
90. Sisson, T. W. & Bacon, C. R. Gas-driven filter pressing in magmas. *Geology* **27**, 613–616 (1999).
91. Parmigiani, A., Huber, C. & Bachmann, O. Mush microphysics and the reactivation of crystal-rich magma reservoirs. *Journal of Geophysical Research: Solid Earth* **119**, 6308–6322 (2014).
92. Degruyter, W., Parmigiani, A., Huber, C. & Bachmann, O. How do volatiles escape their shallow magmatic hearth? *Philosophical Transactions of the Royal Society A* **377**, 20180017 (2019).
93. Belien, I. B., Cashman, K. V. & Rempel, A. W. Gas accumulation in particle-rich suspensions and implications for bubble populations in crystal-rich magma. *Earth and Planetary Science Letters* **297**, 133–140 (2010).
94. Huber, C. & Parmigiani, A. A physical model for three-phase compaction in silicic magma reservoirs. *Journal of Geophysical Research: Solid Earth* **123**, 2685–2705 (2018).

95. Lenormand, R., Touboul, E. & Zarcone, C. Numerical models and experiments on immiscible displacements in porous media. *Journal of fluid mechanics* **189**, 165–187 (1988).
96. Jackson, M., Blundy, J. & Sparks, R. Chemical differentiation, cold storage and remobilization of magma in the Earth's crust. *Nature* **564**, 405–409 (2018).
97. Solano, J. M. S., Jackson, M. D., Sparks, R. S. J., Blundy, J. D. & Annen, C. Melt Segregation in Deep Crustal Hot Zones: a Mechanism for Chemical Differentiation, Crustal Assimilation and the Formation of Evolved Magmas. *Journal of Petrology* **53**, 1999–2026 (2012).
98. Boudier, F., Nicolas, A. & Ildefonse, B. Magma chambers in the Oman ophiolite: fed from the top and the bottom. *Earth and Planetary Science Letters* **144**, 239–250 (1996).
99. Carbotte, S. M. *et al.* Stacked sills forming a deep melt-mush feeder conduit beneath Axial Seamount. *Geology* **48**, 693–697 (2020).
100. Bachmann, O. & Bergantz, G. W. Rhyolites and their Source Mushes across Tectonic Settings. *Journal of Petrology* **49**, 2277–2285 (2008).
101. Spiegelman, M., Kelemen, P. B. & Aharonov, E. Causes and consequences of flow organization during melt transport: The reaction infiltration instability in compactible media. *Journal of Geophysical Research: Solid Earth* **106**, 2061–2077 (2001).
102. Lissenberg, C. J. & MacLeod, C. J. A reactive porous flow control on mid-ocean ridge magmatic evolution. *Journal of Petrology* **57**, 2195–2220 (2016).
103. Bouilhol, P., Schmidt, M. & Burg, J.-P. Magma transfer and evolution in channels within the arc crust: the pyroxenitic feeder pipes of Sapat (Kohistan, Pakistan). *Journal of Petrology* **56**, 1309–1342 (2015).
104. Sanfilippo, A., MacLeod, C. J., Tribuzio, R., Lissenberg, C. J. & Zanetti, A. Early-stage melt-rock reaction in a cooling crystal mush beneath a slow-

spreading mid-ocean ridge (IODP Hole U1473A, Atlantis Bank, Southwest Indian Ridge). *Frontiers in Earth Science* **8**, 579138 (2020).

105. Chadam, J., Hoff, D., Merino, E., Ortoleva, P. & Sen, A. Reactive infiltration instabilities. *IMA Journal of Applied Mathematics* **36**, 207–221 (1986).

106. Spiegelman, M. Flow in deformable porous media. Part 1 Simple analysis. *Journal of Fluid Mechanics* **247**, 17–38 (1993).

107. Ryan, A. G., Hansen, L. N., Zimmerman, M. E. & Pistone, M. Melt Migration in Crystal Mushes by Viscous Fingering: Insights From High-Temperature, High-Pressure Experiments. *JGR Solid Earth* **127**, e2022JB024447 (2022).

108. Richter, F. M. & McKenzie, D. Dynamical models for melt segregation from a deformable matrix. *The Journal of Geology* **92**, 729–740 (1984).

109. Seropian, G., Rust, A. & Sparks, R. The gravitational stability of lenses in magma mushes: Confined Rayleigh-Taylor instabilities. *Journal of Geophysical Research: Solid Earth* **123**, 3593–3607 (2018).

110. Connolly, J. & Podladchikov, Y. Y. Decompaction weakening and channeling instability in ductile porous media: Implications for asthenospheric melt segregation. *Journal of Geophysical Research: Solid Earth* **112**, (2007).

111. Riel, N. *et al.* Interaction between mantle-derived magma and lower arc crust: quantitative reactive melt flow modelling using STyx. *Geological Society, London, Special Publications* **478**, 65–87 (2019).

112. Petford, N., Koenders, M. & Clemens, J. D. Igneous differentiation by deformation. *Contributions to Mineralogy and Petrology* **175**, 45 (2020).

113. Carrara, A., Burgisser, A. & Bergantz, G. W. Lubrication effects on magmatic mush dynamics. *Journal of Volcanology and Geothermal Research* **380**, 19–30 (2019).

114. Van der Molen, I. & Paterson, M. Experimental deformation of partially-melted granite. *Contributions to Mineralogy and Petrology* **70**, 299–318 (1979).

115. Ryan, A. G. *et al.* Shear-induced dilation and dike formation during mush deformation. *Earth and Planetary Science Letters* **651**, 119164 (2025).
116. Rosenberg, C. L. & Handy, M. R. Experimental deformation of partially melted granite revisited: implications for the continental crust. *Journal of metamorphic Geology* **23**, 19–28 (2005).
117. Rummel, L., Kaus, B. J., Baumann, T. S., White, R. W. & Riel, N. Insights into the compositional evolution of crustal magmatic systems from coupled petrological-geodynamical models. *Journal of Petrology* **61**, egaa029 (2020).
118. Liu, B. & Lee, C.-T. Fast melt expulsion from crystal-rich mushes via induced anisotropic permeability. *Earth and Planetary Science Letters* **571**, 117113 (2021).
119. Allan, A. S., Morgan, D. J., Wilson, C. J. & Millet, M.-A. From mush to eruption in centuries: assembly of the super-sized Oruanui magma body. *Contributions to Mineralogy and Petrology* **166**, 143–164 (2013).
120. Cembrano, J. & Lara, L. The link between volcanism and tectonics in the southern volcanic zone of the Chilean Andes: a review. *Tectonophysics* **471**, 96–113 (2009).
121. Humphreys, M. & Holness, M. Melt-rich segregations in the Skaergaard Marginal Border Series: Tearing of a vertical silicate mush. *Lithos* **119**, 181–192 (2010).
122. Natland, J. H. & Dick, H. J. Formation of the lower ocean crust and the crystallization of gabbroic cumulates at a very slowly spreading ridge. *Journal of Volcanology and Geothermal Research* **110**, 191–233 (2001).
123. Namur, O., Humphreys, M. C. & Holness, M. B. Lateral reactive infiltration in a vertical gabbroic crystal mush, Skaergaard intrusion, East Greenland. *Journal of Petrology* **54**, 985–1016 (2013).

124. Li, J.-Y., Wang, X.-L., Gu, Z.-D., Wang, D. & Du, D.-H. Geochemical diversity of continental arc basaltic mushy reservoirs driven by reactive melt infiltration. *Communications Earth & Environment* **5**, 109 (2024).
125. Boulanger, M. & France, L. Cumulate formation and melt extraction from mush-dominated magma reservoirs: the melt flush process exemplified at mid-ocean ridges. *Journal of Petrology* **64**, egad005 (2023).
126. Leuthold, J. *et al.* Partial melting of lower oceanic crust gabbro: constraints from poikilitic clinopyroxene primocrysts. *Frontiers in Earth Science* **6**, 15 (2018).
127. Huber, C., Bachmann, O. & Dufek, J. Thermo-mechanical reactivation of locked crystal mushes: Melting-induced internal fracturing and assimilation processes in magmas. *Earth and Planetary Science Letters* **304**, 443–454 (2011).
128. Hepworth, L. N., O'Driscoll, B., Gertisser, R., Daly, J. S. & Emeleus, C. H. Linking in situ crystallization and magma replenishment via sill intrusion in the Rum Western Layered Intrusion, NW Scotland. *Journal of Petrology* **59**, 1605–1642 (2018).
129. Hu, H., Jackson, M. D. & Blundy, J. Melting, compaction and reactive flow: controls on melt fraction and composition change in crustal mush reservoirs. *Journal of Petrology* **63**, egac097 (2022).
130. Kohlstedt, D. L. & Holtzman, B. K. Shearing melt out of the Earth: An experimentalist's perspective on the influence of deformation on melt extraction. *Annual Review of Earth and Planetary Sciences* **37**, 561–593 (2009).
131. Smith, D. J. Clinopyroxene precursors to amphibole sponge in arc crust. *Nature Communications* **5**, 4329 (2014).
132. Lissenberg, C. J., MacLeod, C. J., Howard, K. A. & Godard, M. Pervasive reactive melt migration through fast-spreading lower oceanic crust (Hess Deep, equatorial Pacific Ocean). *Earth and Planetary Science Letters* **361**, 436–447 (2013).

133. Zhang, W.-Q. & Liu, C.-Z. Crust-scale reactive porous flow revealed by the brown amphibole in the IODP hole U1473A gabbros, Southwest Indian Ridge. *Lithos* **450**, 107209 (2023).
134. Gleeson, M. L., Lissenberg, C. J. & Antoshechkina, P. M. Porosity evolution of mafic crystal mush during reactive flow. *Nature Communications* **14**, 3088 (2023).
135. Yang, A. Y., Wang, C., Liang, Y. & Lissenberg, C. J. Reaction between mid-ocean ridge basalt and lower oceanic crust: An experimental study. *Geochemistry, Geophysics, Geosystems* **20**, 4390–4407 (2019).
136. Blundy, J. Chemical Differentiation by Mineralogical Buffering in Crustal Hot Zones. *Journal of Petrology* **63**, egac054 (2022).
137. Müntener, O. & Ulmer, P. Arc crust formation and differentiation constrained by experimental petrology. *American Journal of Science* **318**, 64–89 (2018).
138. Blatter, D. L., Sisson, T. W. & Hankins, W. B. Voluminous arc dacites as amphibole reaction-boundary liquids. *Contributions to Mineralogy and Petrology* **172**, 1–37 (2017).
139. Blatter, D. L., Sisson, T. W. & Hankins, W. B. Voluminous arc dacites as amphibole reaction-boundary liquids. *Contributions to Mineralogy and Petrology* **172:27**, 27 (2017).
140. Ulmer, P., Kaegi, R. & Müntener, O. Experimentally derived intermediate to silica-rich arc magmas by fractional and equilibrium crystallization at 1· 0 GPa: an evaluation of phase relationships, compositions, liquid lines of descent and oxygen fugacity. *Journal of Petrology* **59**, 11–58 (2018).
141. Hepworth, L. N. *et al.* Rapid crystallization of precious-metal-mineralized layers in mafic magmatic systems. *Nature Geoscience* **13**, 375–381 (2020).
142. Lissenberg, C. J. & Dick, H. J. Melt–rock reaction in the lower oceanic crust and its implications for the genesis of mid-ocean ridge basalt. *Earth and Planetary Science Letters* **271**, 311–325 (2008).

143. Gudmundsson, A. The mechanics of large volcanic eruptions. *Earth-Science Reviews* **163**, 72–93 (2016).

144. Cooper, K. M. Time scales and temperatures of crystal storage in magma reservoirs: implications for magma reservoir dynamics. *Philosophical Transactions of the Royal Society A* **377**, 20180009 (2019).

145. Cooper, K. M. & Kent, A. J. Rapid remobilization of magmatic crystals kept in cold storage. *Nature* **506**, 480–483 (2014).

146. Molina, P. G. *et al.* Protracted late magmatic stage of the Caleu pluton (central Chile) as a consequence of heat redistribution by diking: Insights from zircon data and thermal modeling. *Lithos* **227**, 255–268 (2015).

147. Bachmann, O., Dungan, M. A. & Lipman, P. W. The Fish Canyon magma body, San Juan volcanic field, Colorado: rejuvenation and eruption of an upper-crustal batholith. *Journal of Petrology* **43**, 1469–1503 (2002).

148. Spera, F. J. & Bohrson, W. A. Rejuvenation of crustal magma mush: a tale of multiply nested processes and timescales. *American Journal of Science* **318**, 90–140 (2018).

149. Huber, C., Bachmann, O. & Manga, M. Two competing effects of volatiles on heat transfer in crystal-rich magmas: thermal insulation vs defrosting. *Journal of Petrology* **51**, 847–867 (2010).

150. Huber, C., Bachmann, O. & Dufek, J. The limitations of melting on the reactivation of silicic mushes. *Journal of Volcanology and Geothermal Research* **195**, 97–105 (2010).

151. Passmore, E., Maclennan, J., Fitton, G. & Thordarson, T. Mush Disaggregation in Basaltic Magma Chambers: Evidence from the AD 1783 Laki Eruption. *Journal of Petrology* **53**, 2593–2623 (2012).

152. Moore, A., Coogan, L., Costa, F. & Perfit, M. Primitive melt replenishment and crystal-mush disaggregation in the weeks preceding the 2005–2006 eruption 9 50′ N, EPR. *Earth and Planetary Science Letters* **403**, 15–26 (2014).

153. Christopher, T. E. *et al.* Crustal-scale degassing due to magma system destabilization and magma-gas decoupling at Soufriere Hills Volcano, Montserrat. *Geochemistry, Geophysics, Geosystems* **16**, 2797–2811 (2015).
154. Carrara, A. & Bergantz, G. W. Numerical simulations of the mingling caused by a magma intruding a resident mush. *Volcanica* **7**, 89–104 (2024).
155. Bachmann, O. & Bergantz, G. W. Gas percolation in upper-crustal silicic crystal mushes as a mechanism for upward heat advection and rejuvenation of near-solidus magma bodies. *Journal of Volcanology and Geothermal Research* **149**, 85–102 (2006).
156. Connolly, J. A. D. & Podladchikov, Y. Y. A Hydromechanical Model for Lower Crustal Fluid Flow. in *Metasomatism and the Chemical Transformation of Rock* 599–658 (Springer Berlin Heidelberg, Berlin, Heidelberg, 2013). doi:10.1007/978-3-642-28394-9_14.
157. Spera, F. J. & Bohrson, W. A. Energy-constrained open-system magmatic processes I: General model and energy-constrained assimilation and fractional crystallization (EC-AFC) formulation. *Journal of Petrology* **42**, 999–1018 (2001).
158. Burgisser, A. & Bergantz, G. W. A rapid mechanism to remobilize and homogenize highly crystalline magma bodies. *Nature* **471**, 212–215 (2011).
159. Hickey-Vargas, R., Abdollahi, M. J., Parada, M. A., López-Escobar, L. & Frey, F. A. Crustal xenoliths from Calbuco Volcano, Andean Southern Volcanic Zone: implications for crustal composition and magma-crust interaction. *Contributions to Mineralogy and Petrology* **119**, 331–344 (1995).
160. Costa, F., Dungan, M. A. & Singer, B. S. Hornblende- and Phlogopite-Bearing Gabbroic Xenoliths from Volcán San Pedro (36°S), Chilean Andes: Evidence for Melt and Fluid Migration and Reactions in Subduction-Related Plutons. *J. Petrology* **43**, 219–241 (2002).
161. Clemens, J., Stevens, G., Frei, D. & Joseph, C. Origins of cryptic variation in the Ediacaran–Fortunian rhyolitic ignimbrites of the Saldanha Bay Volcanic

Complex, Western Cape, South Africa. *Contributions to Mineralogy and Petrology* **172**, 1–23 (2017).

162. Humphreys, M. C. *et al.* Unravelling the complexity of magma plumbing at Mount St. Helens: a new trace element partitioning scheme for amphibole. *Contributions to Mineralogy and Petrology* **174**, 1–15 (2019).

163. Hughes, G. E., Petrone, C. M., Downes, H., Varley, N. R. & Hammond, S. J. Mush remobilisation and mafic recharge: A study of the crystal cargo of the 2013–17 eruption at Volcán de Colima, Mexico. *Journal of Volcanology and Geothermal Research* **416**, 107296 (2021).

164. Klaver, M., Blundy, J. D. & Vroon, P. Z. Generation of arc rhyodacites through cumulate-melt reactions in a deep crustal hot zone: evidence from Nisyros volcano. *Earth and Planetary Science Letters* **497**, 169–180 (2018).

165. Erdmann, S., Scaillet, B. & Kellett, D. Textures of peritectic crystals as guides to reactive minerals in magmatic systems: new insights from melting experiments. *Journal of Petrology* **53**, 2231–2258 (2012).

166. Watts, K. E., Bindeman, I. N. & Schmitt, A. K. Crystal scale anatomy of a dying supervolcano: an isotope and geochronology study of individual phenocrysts from voluminous rhyolites of the Yellowstone caldera. *Contrib Mineral Petrol* **164**, 45–67 (2012).

167. Claiborne, L. L. *et al.* Tracking magmatic processes through Zr/Hf ratios in rocks and Hf and Ti zoning in zircons: an example from the Spirit Mountain batholith, Nevada. *Mineralogical Magazine* **70**, 517–543 (2006).

168. Cooper, K. M. Timescales of crustal magma reservoir processes: insights from U-series crystal ages. *Geological Society, London, Special Publications* **422**, 141–174 (2015).

169. Andersen, N. L., Jicha, B. R., Singer, B. S. & Hildreth, W. Incremental heating of Bishop Tuff sanidine reveals preeruptive radiogenic Ar and rapid remobilization

from cold storage. *Proceedings of the National Academy of Sciences* **114**, 12407–12412 (2017).

170. Cooper, G. F., Morgan, D. J. & Wilson, C. J. Rapid assembly and rejuvenation of a large silicic magmatic system: Insights from mineral diffusive profiles in the Kidnappers and Rocky Hill deposits, New Zealand. *Earth and Planetary Science Letters* **473**, 1–13 (2017).

171. Weber, G., Blundy, J. & Bevan, D. Mush Amalgamation, Short Residence, and Sparse Detectability of Eruptible Magma Before Andean Super-Eruptions. *Geochemistry, Geophysics, Geosystems* **24**, e2022GC010732 (2023).

172. Chamberlain, K. J., Morgan, D. J. & Wilson, C. J. N. Timescales of mixing and mobilisation in the Bishop Tuff magma body: perspectives from diffusion chronometry. *Contrib Mineral Petrol* **168**, 1034 (2014).

173. Costa, F., Andreastuti, S., de Maisonneuve, C. B. & Pallister, J. S. Petrological insights into the storage conditions, and magmatic processes that yielded the centennial 2010 Merapi explosive eruption. *Journal of Volcanology and Geothermal Research* **261**, 209–235 (2013).

174. Morgado, E. *et al.* Old magma and a new, intrusive trigger: using diffusion chronometry to understand the rapid-onset Calbuco eruption, April 2015 (Southern Chile). *Contributions to Mineralogy and Petrology* **174**, 1–11 (2019).

175. Barboni, M. *et al.* Warm storage for arc magmas. *Proc. Natl. Acad. Sci. U.S.A.* **113**, 13959–13964 (2016).

176. Jollands, M. C., Bloch, E. & Müntener, O. New Ti-in-quartz diffusivities reconcile natural Ti zoning with time scales and temperatures of upper crustal magma reservoirs. *Geology* **48**, 654–657 (2020).

177. Grocolas, T., Bloch, E. M., Bouvier, A.-S. & Müntener, O. Diffusion of Sr and Ba in plagioclase: Composition and silica activity dependencies, and application to volcanic rocks. *Earth and Planetary Science Letters* **651**, 119141 (2025).

178. Cooper, G. F., Wilson, C. J., Millet, M.-A., Baker, J. A. & Smith, E. G. Systematic tapping of independent magma chambers during the 1 Ma Kidnappers supereruption. *Earth and Planetary Science Letters* **313**, 23–33 (2012).
179. Mallea-Lillo, F., Parada, M. A., Morgado, E., Contreras, C. & Hübner, D. Contrasting sources and conditions of shallow magmatic reservoirs of the Fui Group small eruptive centres associated with the Liquiñe-Ofqui Fault Zone (Chilean Andes). *Journal of South American Earth Sciences* **117**, 103875 (2022).
180. Huber, C., Bachmann, O. & Manga, M. Homogenization processes in silicic magma chambers by stirring and mushification (latent heat buffering). *Earth and Planetary Science Letters* **283**, 38–47 (2009).
181. Booth, C. A., Jackson, M. D., Sparks, R. S. J. & Rust, A. C. Source reservoir controls on the size, frequency, and composition of large-scale volcanic eruptions. *Science Advances* **10**, eadd1595 (2024).
182. Spera, F. Thermal evolution of plutons: a parameterized approach. *Science* **207**, 299–301 (1980).
183. Farner, M. J. & Lee, C.-T. A. Effects of crustal thickness on magmatic differentiation in subduction zone volcanism: A global study. *Earth and Planetary Science Letters* **470**, 96–107 (2017).
184. Bea, F. The sources of energy for crustal melting and the geochemistry of heat-producing elements. *Lithos* **153**, 278–291 (2012).
185. Schaen, A. J. *et al.* Transient rhyolite melt extraction to produce a shallow granitic pluton. *Sci. Adv.* **7**, eabf0604 (2021).
186. Annen, C., Blundy, J. & Sparks, R. The genesis of intermediate and silicic magmas in deep crustal hot zones. *Journal of Petrology* **47**, 505–539 (2006).
187. Walker, B. A., Grunder, A. L. & Wooden, J. L. Organization and thermal maturation of long-lived arc systems: Evidence from zircons at the Aucanquilcha volcanic cluster, northern Chile. *Geology* **38**, 1007–1010 (2010).

188. Grunder, A. L., Klemetti, E. W., Feeley, T. C. & McKee, C. M. Eleven million years of arc volcanism at the Aucanquilcha Volcanic Cluster, northern Chilean Andes: implications for the life span and emplacement of plutons. *Earth and Environmental Science Transactions of the Royal Society of Edinburgh* **97**, 415–436 (2008).

189. Dufek, J. & Bergantz, G. Lower crustal magma genesis and preservation: a stochastic framework for the evaluation of basalt–crust interaction. *Journal of Petrology* **46**, 2167–2195 (2005).

190. Hawkesworth, C. *et al.* Time scales of crystal fractionation in magma chambers—integrating physical, isotopic and geochemical perspectives. *Journal of Petrology* **41**, 991–1006 (2000).

191. Lissenberg, C. J., Rioux, M., Shimizu, N., Bowring, S. A. & Mével, C. Zircon dating of oceanic crustal accretion. *Science* **323**, 1048–1050 (2009).

192. Laporte, D., Rapaille, C. & Provost, A. Wetting angles, equilibrium melt geometry, and the permeability threshold of partially molten crustal protoliths. *Granite: from segregation of melt to emplacement fabrics* 31–54 (1997).

193. Walker Jr, B. A., Bergantz, G. W., Otamendi, J. E., Ducea, M. N. & Cristofolini, E. A. A MASH zone revealed: the mafic complex of the Sierra Valle Fértil. *Journal of Petrology* **56**, 1863–1896 (2015).

194. Schaltegger, U. *et al.* Zircon petrochronology and 40Ar/39Ar thermochronology of the Adamello Intrusive Suite, N. Italy: monitoring the growth and decay of an incrementally assembled magmatic system. *Journal of Petrology* **60**, 701–722 (2019).

195. Morgan, C., Morgado, E., Parada, M.-Á., Brahm, R. & Mallea-Lillo, F. Two-stage evolution of a bimodal reservoir: The case of Holocene lavas of the Lanín composite volcano, Southern Volcanic Zone, Chile. *Journal of South American Earth Sciences* **133**, 104697 (2024).

196. Gutiérrez, F. & Parada, M. A. Numerical modeling of time-dependent fluid dynamics and differentiation of a shallow basaltic magma chamber. *Journal of Petrology* **51**, 731–762 (2010).
197. Wark, D., Kempter, K. & McDowell, F. Evolution of waning, subduction-related magmatism, northern Sierra Madre Occidental, Mexico. *Geological Society of America Bulletin* **102**, 1555–1564 (1990).
198. Godoy, B. *et al.* Linking the mafic volcanism with the magmatic stages during the last 1 Ma in the main volcanic arc of the Altiplano-Puna Volcanic Complex (Central Andes). *Journal of South American Earth Sciences* **95**, 102295 (2019).
199. Moore, N. E., Grunder, A. L., Bohrson, W. A., Carlson, R. W. & Bindeman, I. N. Changing Mantle Sources and the Effects of Crustal Passage on the Steens Basalt, SE Oregon: Chemical and Isotopic Constraints. *Geochem Geophys Geosyst* **21**, e2020GC008910 (2020).
200. Broderick, C. *et al.* Linking the thermal evolution and emplacement history of an upper-crustal pluton to its lower-crustal roots using zircon geochronology and geochemistry (southern Adamello batholith, N. Italy). *Contrib Mineral Petrol* **170**, 28 (2015).
201. Loucks, R. R. Deep entrapment of buoyant magmas by orogenic tectonic stress: Its role in producing continental crust, adakites, and porphyry copper deposits. *Earth-Science Reviews* **220**, 103744 (2021).
202. Hartung, E., Weber, G. & Caricchi, L. The role of H2O on the extraction of melt from crystallising magmas. *Earth and Planetary Science Letters* **508**, 85–96 (2019).
203. Jerram, D. A., Cheadle, M. J. & Philpotts, A. R. Quantifying the building blocks of igneous rocks: are clustered crystal frameworks the foundation? *Journal of Petrology* **44**, 2033–2051 (2003).

204. Philpotts, A. R., Shi, J. & Brustman, C. Role of plagioclase crystal chains in the differentiation of partly crystallized basaltic magma. *Nature* **395**, 343–346 (1998).

205. Rudge, J. F., Holness, M. B. & Smith, G. C. Quantitative textural analysis of packings of elongate crystals. *Contributions to Mineralogy and Petrology* **156**, 413–429 (2008).

206. Saar, M. O., Manga, M., Cashman, K. V. & Fremouw, S. Numerical models of the onset of yield strength in crystal–melt suspensions. *Earth and Planetary Science Letters* **187**, 367–379 (2001).

207. Nolan, G. & Kavanagh, P. Computer simulation of random packings of spheres with log-normaldistributions. *Powder technology* **76**, 309–316 (1993).

208. He, D., Ekere, N. N. & Cai, L. Computer simulation of random packing of unequal particles. *Physical review E* **60**, 7098 (1999).

209. Nield, D. A. & Bejan, A. *Convection in Porous Media*. vol. 3 (Springer, 2006).

210. Zakirov, T. R. & Khramchenkov, M. G. Prediction of permeability and tortuosity in heterogeneous porous media using a disorder parameter. *Chemical Engineering Science* **227**, 115893 (2020).

211. Röding, M., Ma, Z. & Torquato, S. Predicting permeability via statistical learning on higher-order microstructural information. *Scientific reports* **10**, 1–17 (2020).

212. Vasseur, J., Wadsworth, Fabian B, Bretagne, E. & Dingwell, Donald B. Universal scaling for the permeability of random packs of overlapping and nonoverlapping particles. *Physical Review E* **105**, L043301 (2022).

213. Hersum, T. Consequences of crystal shape and fabric on anisotropic permeability in magmatic mush. *Contributions to Mineralogy and Petrology* **157**, 285–300 (2009).

214. Vasseur, J., Wadsworth, F. B., Coumans, J. P. & Dingwell, D. B. Permeability of packs of polydisperse hard spheres. *Physical Review E* **103**, 062613 (2021).

215. Bretagne, E., Wadsworth, F. B., Vasseur, J. & Dobson, K. J. A Scaling for the Permeability of Loose Magma Mush Validated Using X-Ray Computed Tomography of Packed Confectionary in 3D and Estimation Methods From 2D Crystal Shapes. *Journal of Geophysical Research: Solid Earth* **128**, e2023JB026795 (2023).

216. Rosenberg, N. & Spera, F. Role of anisotropic and/or layered permeability in hydrothermal convection. *Geophysical Research Letters* **17**, 235–238 (1990).

217. Hunter, R. H. Textural equilibrium in layered igneous rocks. in *Origins of igneous layering* 473–503 (Springer, 1987).

218. Holness, M. B., Humphreys, M. C., Sides, R., Helz, R. T. & Tegner, C. Toward an understanding of disequilibrium dihedral angles in mafic rocks. *Journal of Geophysical Research: Solid Earth* **117**, (2012).

219. Holness, M., Clemens, J. & Vernon, R. How deceptive are microstructures in granitic rocks? Answers from integrated physical theory, phase equilibrium, and direct observations. *Contributions to Mineralogy and Petrology* **173**, 1–18 (2018).

220. Riel, N., Kaus, B. J. P., Green, E. C. R. & Berlie, N. MAGEMin, an Efficient Gibbs Energy Minimizer: Application to Igneous Systems. *Geochem Geophys Geosyst* **23**, e2022GC010427 (2022).

221. Holland, T. J. B., Green, E. C. R. & Powell, R. Melting of Peridotites through to Granites: A Simple Thermodynamic Model in the System KNCFMASHTOCr. *Journal of Petrology* **59**, 881–900 (2018).

222. Grove, T. L. & Kinzler, R. J. Petrogenesis of andesites. *Annual Review of Earth and Planetary Sciences* **14**, 417–454 (1986).

223. Gale, A., Dalton, C. A., Langmuir, C. H., Su, Y. & Schilling, J. The mean composition of ocean ridge basalts. *Geochem Geophys Geosyst* **14**, 489–518 (2013).

224. Plank, T. & Langmuir, C. H. An evaluation of the global variations in the major element chemistry of arc basalts. *Earth and Planetary Science Letters* **90**, 349–370 (1988).

225. Nandedkar, R. H., Ulmer, P. & Müntener, O. Fractional crystallization of primitive, hydrous arc magmas: an experimental study at 0.7 GPa. *Contrib Mineral Petrol* **167**, 1015 (2014).

226. Villiger, S. The Liquid Line of Descent of Anhydrous, Mantle-Derived, Tholeiitic Liquids by Fractional and Equilibrium Crystallization--an Experimental Study at 1.0 GPa. *Journal of Petrology* **45**, 2369–2388 (2004).

227. Villiger, S., Ulmer, P. & Muntener, O. Equilibrium and Fractional Crystallization Experiments at 0.7 GPa; the Effect of Pressure on Phase Relations and Liquid Compositions of Tholeiitic Magmas. *Journal of Petrology* **48**, 159–184 (2006).

Display items

Box 1. Physical properties of crystal mushes

Porosity and crystal content – In crystal mushes, the solids form an interconnected framework and melt can percolate through the framework until the percolation threshold **[G]** is reached. The initial solid fraction of a mush depends on many factors including crystal size and shape (i.e. aspect ratio). Structural analysis of natural crystal mush frameworks typically suggests relatively low initial crystal fraction (ϕ), down to $\phi = 0.2$ (ref. [203]). This is consistent with high-temperature basalt partial melting experiments where rock strength is maintained by chains of interconnected plagioclase crystals, until a crystal fraction of ~0.3[204]. Analogue experiments to create random, loosely packed mushes show that solid fraction decreases with increasing friction and particle aspect ratio[55,205]. Numerically simulated mushes of anisotropic cuboids (approximating plagioclase shapes) can also have very low solid fraction, down to <0.2 depending on crystal shape[59,206]. The crystal fraction of a natural crystal mush can therefore be locally heterogeneous and will increase with increasing crystal size variability[207,208]. These complexities have important rheological impacts. In particular, crystal mush behaviour is commonly described relative to a rheologically locked or 'jammed' state, but there is clearly no fixed crystal fraction at which this occurs: it depends strongly on crystal shape and size distribution.

Permeability – Interstitial liquid can move through the connected pore space of a crystal mush. The rate of melt flow depends on the pressure gradient that drives it (which may arise from buoyancy or external stresses), the melt viscosity, and the geometry of the pore space. These characteristics are captured by the permeability, which is typically described using Darcy's law.

Flow velocity increases with decreasing melt viscosity, increased pressure gradient, and increased permeability[209]. For a mush of spherical particles, the permeability is controlled by the crystal fraction and grainsize[69,209,210], but this can be generalised by instead considering the specific surface areas of the solid crystal framework[211,212], which describes mushes with a significant size distribution or varied shapes[212–215]. Importantly, for natural crystal mushes, permeability will be anisotropic (**Figure 2a**) if there is a crystal fabric, substantial modal layering, or active deformation[118,213,216].

Crystal shape and textural equilibration - Crystals that are growing freely from a melt at low undercooling typically have a compact, euhedral crystal shape. However, that euhedral growth shape is not *texturally* equilibrated with adjacent crystals in a mush, or with the interstitial melt[24,67,217]. Textural equilibration (sometimes described as maturation) in the presence of melt creates smoothly curving melt films on two- and three-grain boundaries[68,192,218] and eventually leads to the formation of equilibrium solid-melt dihedral angles[24,51]. The textural equilibration process is largely diffusive[219] and therefore depends on mush temperature and the composition of both melt and crystals. Prolonged crystal mush storage permits textural equilibration to progress through coarsening and diffusive readjustment of crystal boundaries. Textural equilibration can substantially modify both the texture and physical properties of the mush, most importantly the permeability and percolation threshold[68].

Figures

Figure 1. Schematic mush cross-section. Schematic mush cross-section for a cooling intrusion, drawing on direct observations of crystal mush sampled by drilling (Makaopuhi lava lake[33]) but not intended to be prescriptive of a particular system. Left, the distribution of crystals within a mush as a function of depth. Right, the crystal fraction, temperature and melt composition of a mush. Insets show illustrative mush textures with tabular primocrysts (brown), a space-filling, interstitial phase (pale grey) and melt (darker grey). The dashed line schematically indicates the transition from magma to mush. Depth scale is also schematic and could be a few tens of metres from top to bottom, but more broadly is determined by the heat balance across the mush (including country rock and intrusion temperature, extent of hydrothermal cooling, as well as the relationship between temperature and melt fraction for the melt of interest).

Figure 2. Mush compaction. (a, b) 3D visualisation of porosity reduction through mechanical mush consolidation in the form of translation and rotation (thin black arrows) of individual crystals within an initially loosely packed mush, in response to applied stress (thick black arrows). This results in shape preferred alignment (as shown) in the case of anisotropic crystals. (c) Schematic representation of composite mush rheology (orange line) including contributions from mechanical consolidation (dashed line) and viscous compaction (solid line), after Ref. 53. ϕ_m = maximum packing fraction. Compaction occurs primarily by mechanical consolidation at higher melt fractions > ϕ_m and by viscous compaction at low melt fractions < ϕ_m. (d) Continuous model for liquid-solid compaction length for two-phase flow from porous flow regime (accommodated by viscous compaction at melt fractions < ϕ_m and by melt locliasation between ϕ_m and ϕ_{dis}, the porosity at which mush disaggregates) to suspension flow (crystal settling), after Ref. 48. (e) Cross-polarised photomicrograph showing textural

evidence used to infer viscous compaction, including deformation twinning and mechanical bending (asterisks). Pl, plagioclase; cpx, clinopyroxene; ol, olivine. (f) Cross-polarised photomicrograph showing textural evidence used to infer melt convection, in the form of constant composition rim growth (arrows; after ref. 74).

Figure 3. Reactive melt infiltration. (a) Schematic illustration of grain-scale reaction-infiltration of melt into a matrix of A+B (after Ref. 130). Melt (yellow) undersaturated in phase A (dark blue) infiltrates the mush (red arrows) and reacts with the solid matrix, causing dissolution of A and reprecipitation of B with a new composition. Reactive infiltration takes on a channelised form (white dashed lines). (b) Chondrite-normalised (N) trace element compositions of clinopyroxene from global mid-ocean ridges are largely inconsistent with fractional crystallisation (grey solid arrow) but can be reproduced through reactive melt flow (blue dashed arrow, with a solid modal assemblage of 7.5% olivine (ol) + 43.5% plagioclase (pl) + 49% clinopyroxene (cpx); black dotted arrow, with a solid modal assemblage of 80% cpx + 20% pl, updated after Ref. 102). Circles are data from the East Pacific Rise; triangles, Mid-Atlantic Ridge; squares, South West Indian Ridge.

Figure 4. Mush disaggregation at different scales. (a) Macro-scale Rayleigh-Taylor instabilities may cause plumes of crystal-rich material to descend from mush (red) intruded or underplated by new magma (yellow). (b) Grain-scale disaggregation of mush adjacent to new melt-rich layer (yellow) results in generation of antecrystic crystal cargo in extracted magma. The glomerocryst represents a disaggregated fragment of the mush and shows evidence of dissolution at internal boundaries (arrows) and overgrowth rims that are common to all grains. Hbl, hornblende; pl, plagioclase.

Figure 5. Thermal maturity and crustal magmatic systems. The lifetime of a crustal magmatic system. Temperature is shown on the axis next to each panel. Curving blue arrows indicate hydrothermal circulation. Inset schematic illustrates possible textural features for a new mush developed at each stage. (a) Thermally maturing systems see only localised heat and partial melting and little crustal assimilation. Individual intrusions cool quickly with unequilibrated textures. (b) Thermally mature systems show generally warm crustal temperatures leading to wide-spread mush and significant assimilation and a complex crystal cargo. Textures are more equilibrated and equant following repeated intrusion, resorption, rejuvenation and recrystallisation. Evolved magma is emplaced at mid- to upper-crustal levels. (c) Waning systems retain some of the complex crystal cargo but revert to more localised heat distribution and lower overall ambient temperatures.

Figure 6. Temperature vs melt fraction for different melts. Temperature vs melt fraction trends calculated for wet (dashed lines) and dry (solid lines) melts using the thermodynamic Gibbs free energy minimization package MAGEMin[220] with the Thermocalc igneous thermodynamic database[221]. We assume that wet melts contain 2 wt.% H_2O at their liquidus temperature. Fractional crystallization is simulated under QFM (quartz-fayalite-magnetite equilibrium) oxygen fugacity conditions at a pressure of 0.5 GPa, using 5 °C temperature increments and taking the residue as the new bulk composition for the next step. The andesite starting composition is from Ref. [222], the tholeiite starting composition is from Ref. [223] and the arc basalt starting composition is from Ref. [224]. Experimental constraints for tholeiite and arc basalt are also shown for comparison[225–227].

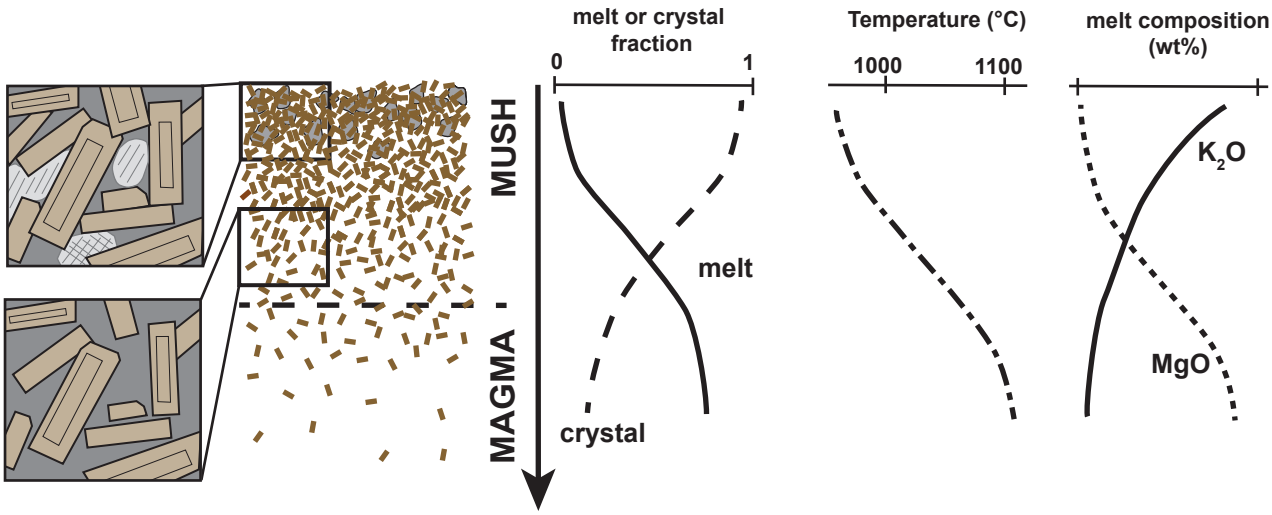

Figure 1. Schematic mush cross-section

Schematic mush cross-section for a cooling intrusion, drawing on direct observations of crystal mush sampled by drilling (Makaopuhi lava lake [Helz 1980]) but not intended to be prescriptive of a particular system.

Depth scale is also schematic and could be a few tens of metres [Helz 1980] but more broadly is determined by the heat balance across the mush (including country rock and intrusion temperature, extent of hydrothermal cooling, as well as the relationship between temperature and melt fraction for the melt of interest).

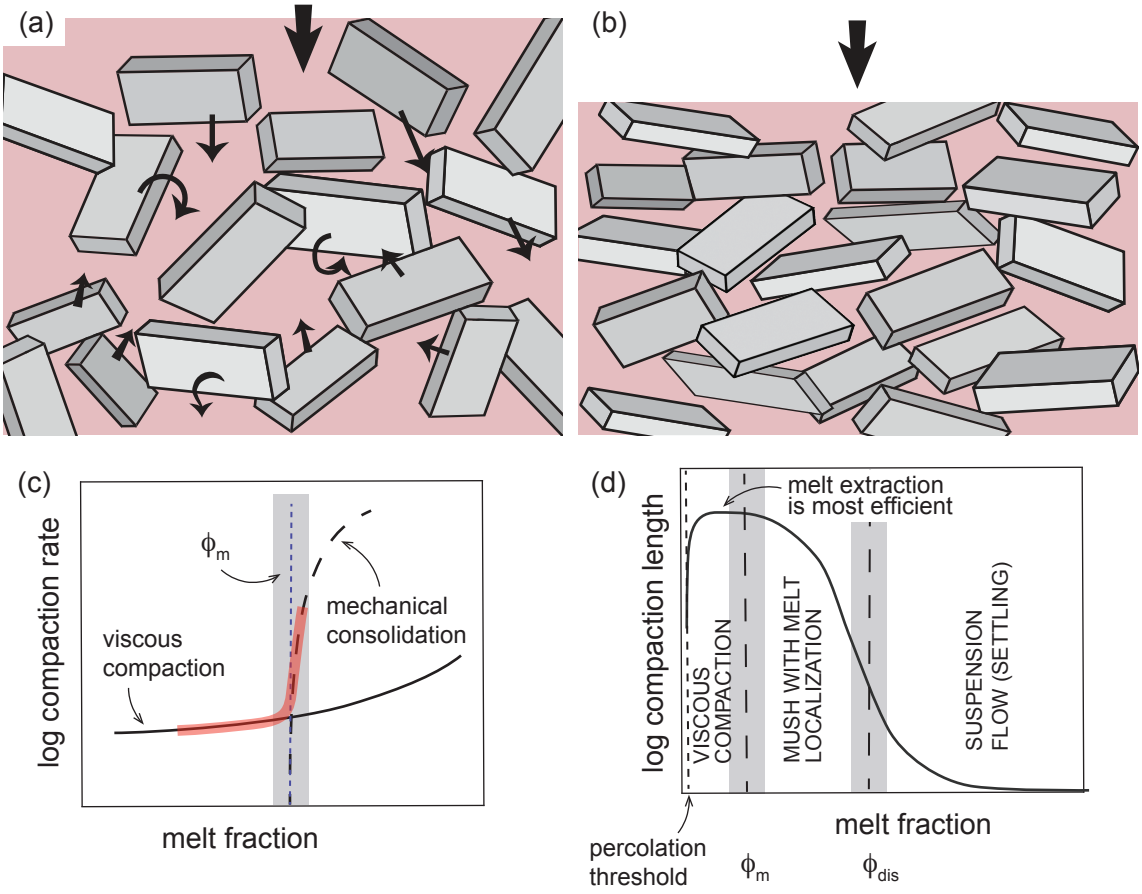

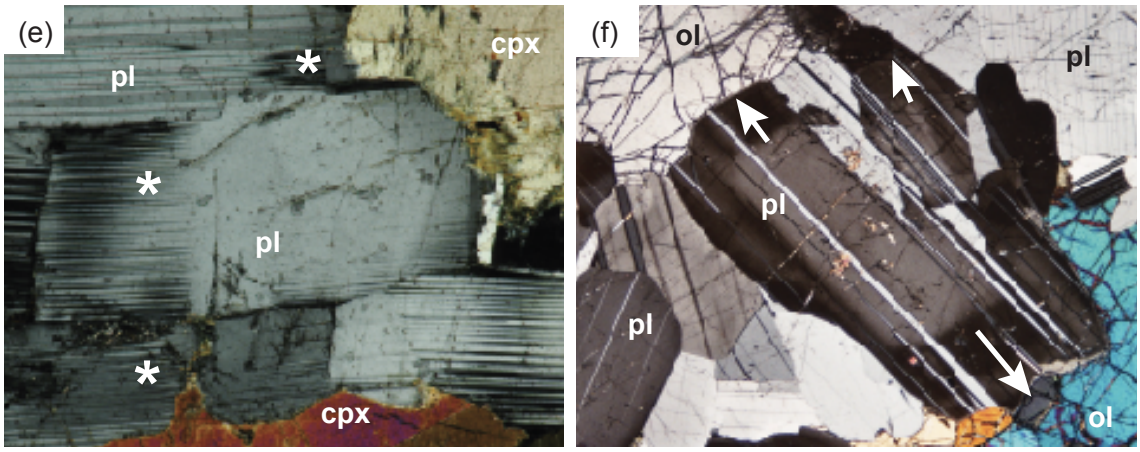

Figure 2. Mush compaction
(a, b) 3D visualisation of porosity reduction through mechanical mush consolidation in the form of translation and rotation (thin black arrows) of individual crystals within an initially loosely packed mush. Shape preferred alignment results in the case of anisotropic crystals. (c) Cross-polarised photomicrograph showing textural evidence used to infer viscous compaction, including deformation twinning and mechanical bending (stars). (d) Cross-polarised photomicrograph showing textural evidence used to infer melt convection, in the form of constant composition rim growth (arrows, after Ref. 74). (e) Porosity reduction occurs by mechanical consolidation at higher melt fractions and by viscous compaction at low melt fractions, after Ref. 53. (f) Continuous model for liquid-solid compaction length for two-phase flow from porous flow regime (accommodated by viscous compaction) to suspension flow (crystal settling), after Ref. 48. ϕ_m = maximum packing fraction, ϕ_{dis} = porosity at which mush disaggregates.

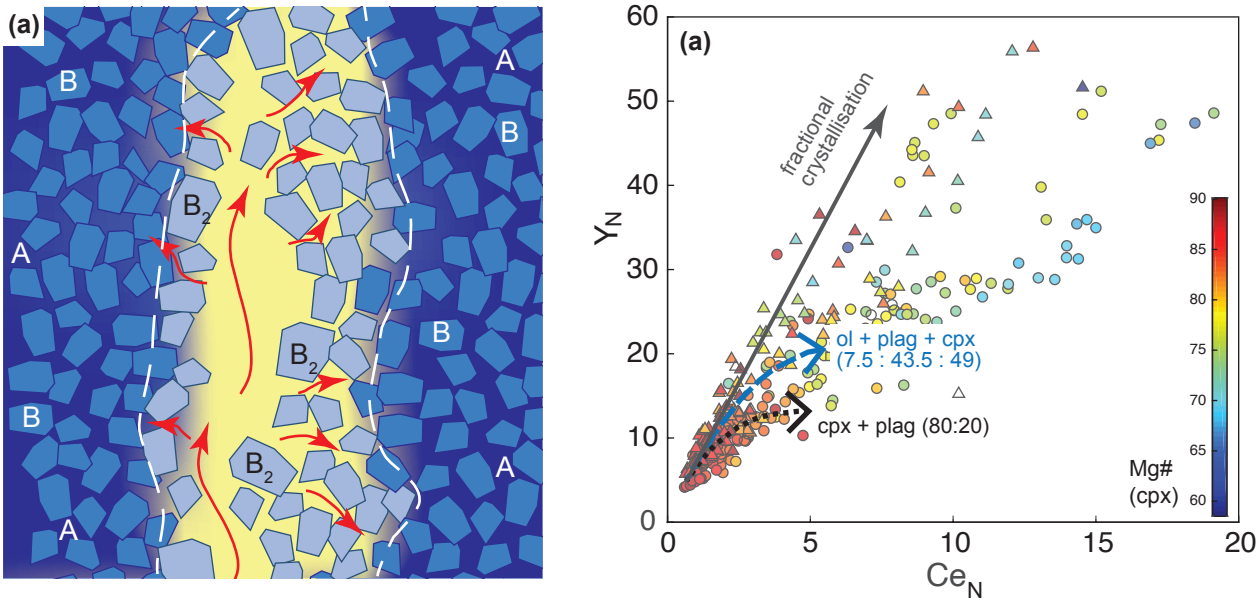

Figure 3. Reactive melt infiltration.

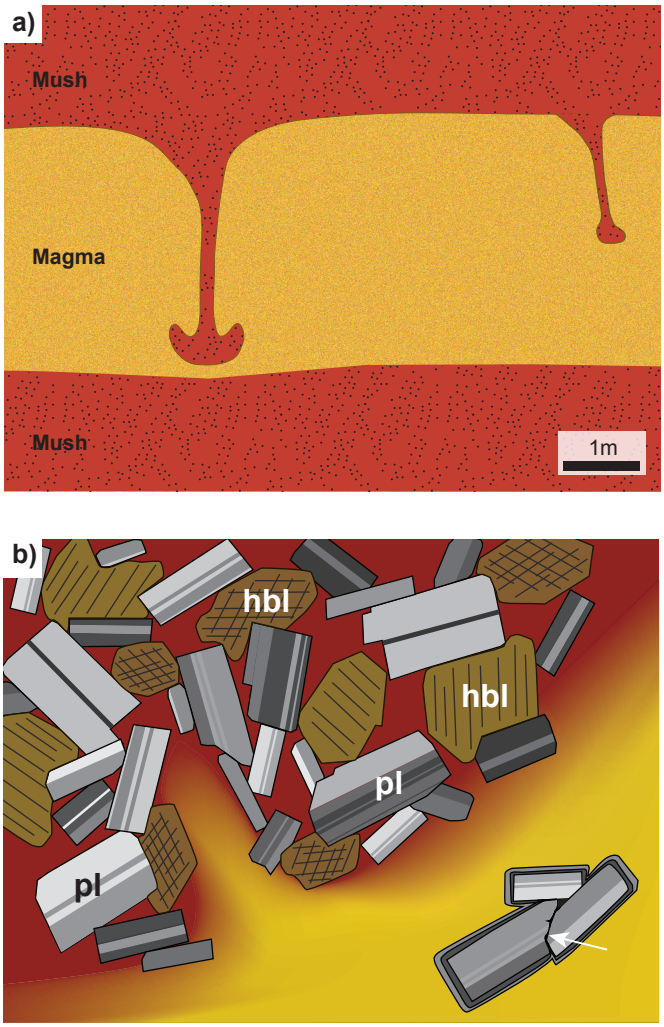

Figure 4. Mush disaggregation at different scales.
(a) Macro-scale Rayleigh-Taylor instabilities from mush intruded or underplated by new magma. (b) Disaggregation at the grainscale adjacent to new melt (yellow) results in generation of glomerocrysts crystal cargo in erupted magmas. Glomerocrysts commonly show evidence of dissolution at internal boundaries (arrows) and common overgrowth rims.

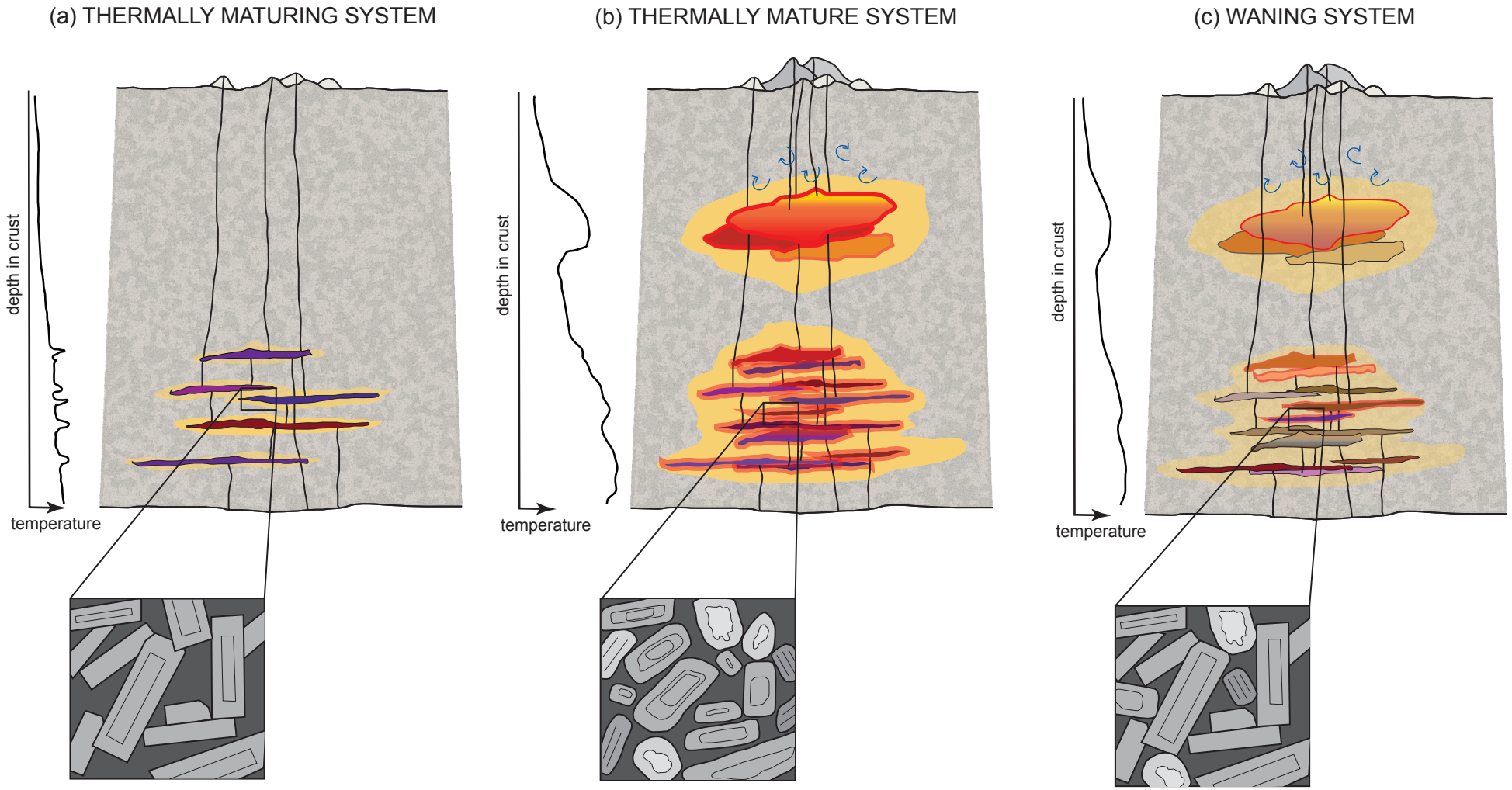

Figure 6. Thermal maturity and crustal magmatic systems
The lifetime of a crustal magmatic system. Temperature is shown on the axis next to each panel. Curving blue arrows indicate hydrothermal circulation. Inset schematic illustrates possible textural features for a new mush developed at each stage. (a) Thermally maturing systems see only localised heat and partial melting and little crustal assimilation. Individual intrusions cool quickly with unequilibrated textures. (b) Thermally mature systems show generally warm crustal temperatures leading to wide-spread mush and significant assimilation and a complex crystal cargo. Textures are more equilibrated and equant following repeated intrusion, resorption, rejuvenation and recrystallisation. Evolved magma is emplaced at mid- to upper-crustal levels. (c) Waning systems retain some of the complex crystal cargo but revert to more localised heat distribution and lower overall ambient temperatures.

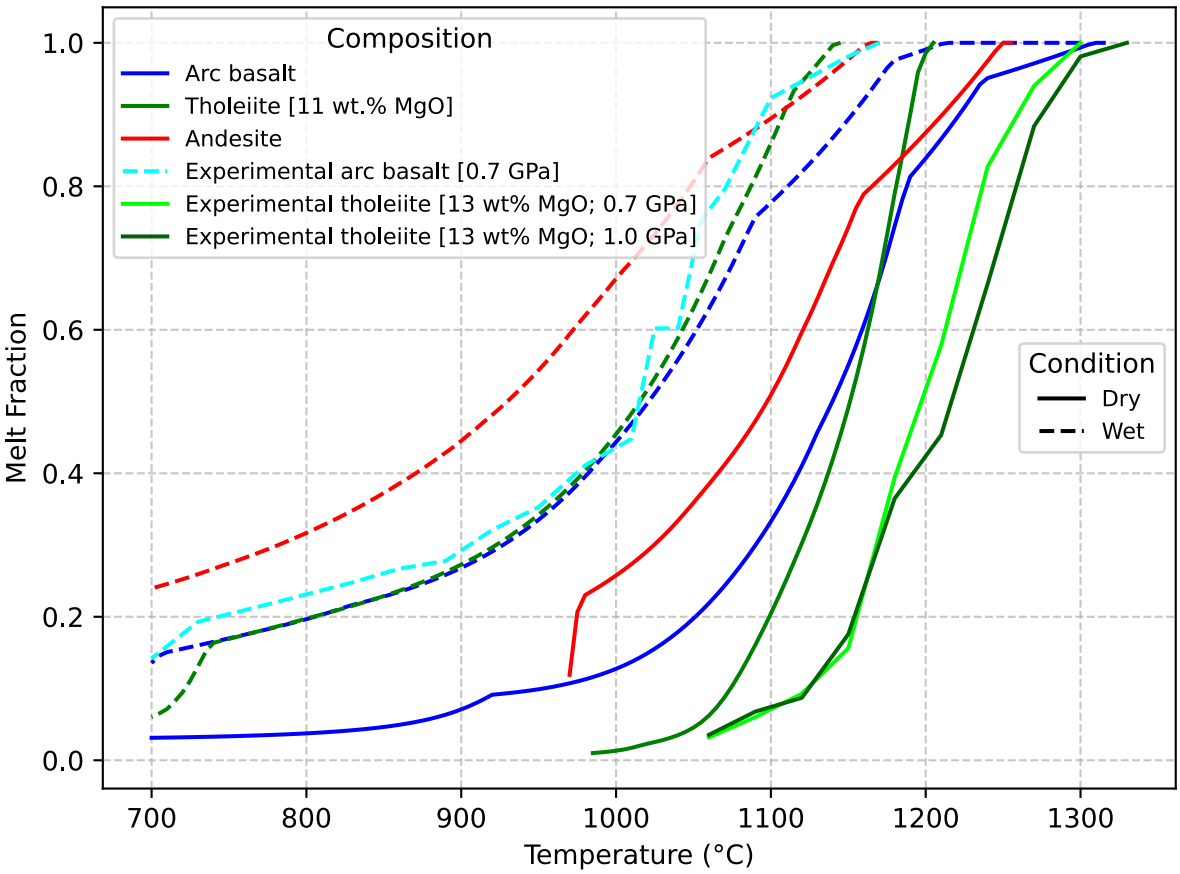

Figure 6. Temperature vs melt fraction for different melts. Temperature vs melt fraction trends calculated for different melts using the thermodynamic Gibbs free energy minimization package MAGEMin[216] with the Thermocalc igneous thermodynamic database[217] . We assume that wet melts contain 2 wt.% H2O at their liquidus temperature and simulate equilibrium crystallization under QFM (quartz-fayalite-magnetite equilibrium) oxygen fugacity conditions at a pressure of 0.5 GPa. The andesite composition is from [218], the tholeiite composition is from [219] and the arc basalt composition is from [220].